Development of an Electrochemical-Surface Enhanced Raman Spectroscopic (EC-SERS) Sensor for Bacterial Screening

By: Taylor Paige Lynk

A Thesis Submitted to

Saint Mary's University, Halifax, Nova Scotia

In Partial Fulfilment of the Requirements for the Degree of

Bachelor of Science with Honours in Chemistry

April 2018, Halifax, Nova Scotia

Co-Supervisor: Dr. Christa Brosseau

Co-Supervisor: Dr. Clarissa Sit

Department Chair: Dr. Robert Singer

Date: April 20, 2018

Certification

Development of an Electrochemical-Surface Enhanced Raman Spectroscopic (EC-SERS) Sensor for Bacterial Screening

By: Taylor Paige Lynk

I hereby certify that this thesis was completed by Taylor Paige Lynk in partial fulfillment of the requirements of the Degree of Bachelor of Science with Honours in Chemistry at Saint Mary's University and I certify that this is truly the original work carried out by Taylor Paige Lynk.

Thesis Co-Supervisor

Dr. Christa L. Brosseau

_____

Thesis Co-Supervisor

Dr. Clarissa Sit

_____

Chairperson of the Chemistry Department

Dr. Robert Singer

_____

Date: April 20, 2018

Abstract

Development of an Electrochemical-Surface Enhanced Raman Spectroscopic (EC-SERS) Sensor for Bacterial Screening

By: Taylor Paige Lynk

The lack of efficiency of current methods for bacterial screening has prompted an increasing interest in developing a cost-effective, rapid and sensitive alternative for applications in all sectors of society. This project aims to explore a new detection platform for bacterial screening by coupling an applied electric potential with surface-enhanced Raman spectroscopy (SERS), a technique termed electrochemical surface-enhanced Raman spectroscopy (EC-SERS). The goal of using this technique is to improve upon the sensitivity and reproducibility of normal SERS to allow for rapid, point-of-need (PON) bacterial detection and identification. This project first shows the EC-SERS characterization of the commonly observed nucleotide breakdown products that dominate the SERS spectra of bacteria: adenine, guanine, xanthine, hypoxanthine, uric acid, 5'-adenosine monophosphate (AMP), and guanosine. This thesis work then concentrates on developing a sample preparation method to be used to study bacteria using EC-SERS for the first time. The results of this project demonstrate the improvement of the SERS spectra of both *E. coli* K-12 and *B. megaterium* bacteria obtained when an electric potential is employed, and highlights the great promise of EC-SERS for use as a fast and affordable bacterial screening method.

April 20, 2018

Acknowledgements

I would like to thank my research supervisors, Dr. Christa Brosseau and Dr. Clarissa Sit for all of their knowledge and guidance during the course of this project. I would especially like to thank Dr. Christa Brosseau for allowing me to work in her research lab for the last number of years and for her constant encouragement. I would also like to thank the current and past Brosseau lab group members: Dalal Alhatab, Najwan Albarghouthi, Natasha Dilkie, Kathleen Allen, Marwa Yasmin, Presley MacMillan, Melanie Davidson, Gaius St. Marie, Shruti Bindesri, Navya Kesevan, and especially Reem Karaballi and Osai Clarke for being my mentors. I would also like to thank Kaitlyn Blatt-Janmaat and the rest of the Sit research group for their assistance with everything bacteria related.

I would also like to extend my appreciation to Alyssa Doué and Darlene Goucher, as well as the entirety of the chemistry department staff for their ongoing assistance. I would like to thank the faculty in the department of chemistry for providing me with my education in chemistry and my appreciation for the subject. Thanks to Dr. Xiang Yang for his help obtaining SEM images and to Carmen Cranley for providing me with all bacterial strains used in this project.

Finally, I would like to thank my friends and family for their love and support, especially my mother, Deborah Lynk, for encouraging me to pursue my dreams.

Table of Contents   Page

List of Figures

532 nm.

List of Tables

List of Abbreviations

AMP   adenosine 5'- monophosphate

PON   point-of-need

AgNP   silver nanoparticles

AuNP   gold nanoparticles

PCR   polymerase chain reaction

RE   reference electrode

CE   counter electrode

WE   working electrode

CV   cyclic voltammetry

IR   Infrared spectroscopy

SERS   surface-enhanced Raman spectroscopy

EC-SERS   electrochemical surface-enhanced Raman spectroscopy

OCP   open circuit potential

SPE   screen printed electrode

IHP   inner Helmoltz plane

OHP   outer Helmoltz plane

Chapter 1: Introduction

1.1 Research Goal

The purpose of this research project is to explore the use of electrochemical-surface enhanced Raman spectroscopy (EC-SERS) for bacterial detection and identification. Current methods for bacterial screening lack time and cost-efficiency, and hence it is critical to develop a bacterial detection platform that combines rapid and cost-effective screening, while maintaining or improving upon the sensitivity and selectivity of current methods. A new bacterial identification technology is needed to improve food safety, expedite patient care, ensure safe water distribution systems, and even investigate bioterrorism threats. A promising candidate for a sensitive, low cost, and rapid technique is an optical method known as surface-enhanced Raman spectroscopy (SERS). Despite initial promise, however, this method has been shown to have major limitations for bacterial screening, the most significant of which is non-reproducible spectra of bacteria that cannot be used to differentiate between strains based on the vibrational signal alone. Ideally, the SERS spectra would provide an identifiable bacterial strain fingerprint, as is commonplace for small molecules. As EC-SERS is known to improve upon the signal produced using normal SERS, it is anticipated that employing an electric potential will allow for signal improvement allowing for higher sensitivity and selectivity for detection of bacteria. The main question this project aims to address is if it is possible to use EC-SERS to enhance the SERS signal of bacteria. If this main goal of bacteria spectral signal improvement is achieved, subsequent goals include fashioning a standard method for EC-SERS analysis of bacteria and using the developed method to differentiate between Gram-positive and Gram-negative bacterial strains using EC-SERS.

1.2 Introduction

Pathogenic bacteria are one of the leading causes of mortality worldwide, resulting in millions of hospitalizations and deaths annually.[1] Efficient bacterial detection is critical in many industries, including the food industry, water and environmental control, clinical diagnosis, and military defence.[1,2] *Salmonella*, *Escherichia coli,* and *Listeria* are among the most negatively impactful strains of bacteria, responsible for many food and waterborne illnesses.[1,2] Other, less life threatening bacterial infections include sexually transmitted diseases such as syphilis, gonorrhea and chlamydia, which are crucial to diagnose early to avoid further population distribution.[1] Clearly, fast and accurate bacterial detection has major implications on human health and safety, and must be carried out in an efficient and cost-effective manner.

The methods currently in place for bacterial detection include polymerase chain reaction (PCR), culture and colony counting, and enzyme-linked immunosorbent assays (ELISA).[2] While these methods are sensitive, selective, and usually conclusive, they can take up to 7 or 8 days to yield results, leaving patients waiting unacceptable amounts of time to receive proper diagnoses and treatment.[2] These currently employed methods also require expensive and specialized instrumentation, adding significant cost to the various sectors that utilize these technologies.[1] A cost-effective, rapid, easy to use, sensitive and selective method for bacterial detection is absolutely necessary to eliminate delays in patient treatment and reduce further spread of bacterial infections and disease.

Raman spectroscopy is a spectroscopic technique based on the inelastic scattering of monochromatic light as a result of the incident radiation's interaction with molecular vibrations.[6] Raman spectroscopy provides valuable molecular fingerprints; however, it is

an inherently weak technique due to the very low proportion of Raman scattered photons.[3] To overcome this weakness, a method termed surface-enhanced Raman spectroscopy (SERS) was developed in the 1970's.[3] SERS benefits from the interaction between incident light and a nanostructured noble metal surface, which causes a significant enhancement of the normal Raman signal.[4] This highly-sensitive technique has gathered great interest, and was therefore considered as a candidate for bacterial detection.

Current methods that employ SERS for bacterial detection involve complicated substrate preparation, including vacuum thermally deposited ultra-thin silver on glass slides[5] and 3D polymer brushes.[6] Additionally, the SERS spectra obtained from bacteria have been shown to be attributed to the metabolites of the purine degradation pathway caused by the rapid onset of the bacterial starvation response; these metabolites include adenine, guanine, AMP, uric acid, xanthine and hypoxanthine.[7] Guanosine has recently been identified as another molecule that contributes to the SERS spectra of bacteria. It has so far not been possible to obtain information about the cell wall of the bacteria, which would be extremely valuable for spectral differentiation of different strains. The outermost section of the cell wall of Gram-positive bacteria consists of a thick layer of peptidoglycan, which also contains lipids and proteins, while the outermost portion of the Gram-negative bacterial cell wall consists of an outer membrane containing lipopolysaccharides.[1] These features of the outer cell wall could help to distinguish between Gram-positive and Gram-negative bacteria, and possibly even between strains. Therefore, it would be extremely beneficial for bacterial screening purposes to obtain spectral peaks from the cell wall of the bacteria as opposed to metabolites released from

the bacteria. Due to the similarity of SERS bacteria spectra reported in literature, it has so far only been possible to differentiate between different strains of bacteria using a barcoding method based on the second derivative of the SERS spectra, coupled with multivariate statistical analysis.[8] The field of SERS therefore requires a way to overcome this limitation in order to acquire more information about bacteria from their corresponding SERS spectra.

Electrochemical-surface enhanced Raman spectroscopy (EC-SERS) couples SERS with the application of an electric potential to the sensor surface in the presence of an electrolyte.[9] This technique allows for an analyte to be detected at a desired applied voltage and simulates a more biologically relevant electric field condition.[9] EC-SERS has been shown to improve upon the normal SERS spectrum of various molecules[9,10] and will therefore be explored for the first time for bacterial screening in this present thesis work.

1.3 Literature Review

1.3.1 Bacteria

Bacteria are ubiquitous and are found throughout our world in water, nature, food, the environment and the human body. An average human carries more than 150 different kinds of bacteria both inside and outside their body.[11] While many of these microorganisms around us carry out important and sometimes essential activities, there are many microorganisms that threaten human life by causing infectious disease. Bacteria-inflicted infectious diseases are responsible for nearly 40% of all deaths worldwide.[12]

Bacteria are unicellular organisms that are typically between 0.5 and 5 microns in size, and can display various shape morphologies such as spherical, cocci, rod-shaped or spiral-shaped.[1] Bacteria can be Gram-positive or Gram-negative, where the two categories vary in terms of the orientation and composition of their cell walls. Figure 1.3.1.1 shows the difference between the two types of bacteria, where Gram-positive bacteria can be seen to have a cell wall that is surrounded in a thick layer of peptidoglycan with an inner cell membrane and lipids on the surface of the cell wall.[1] Gram-negative bacteria are shown to have cell walls that contain a thin layer of peptidoglycan between an inner and outer membrane with lipopolysaccharides associated with their outer surface.[1] Both types of bacteria have various proteins imbedded in their cell walls.[1]
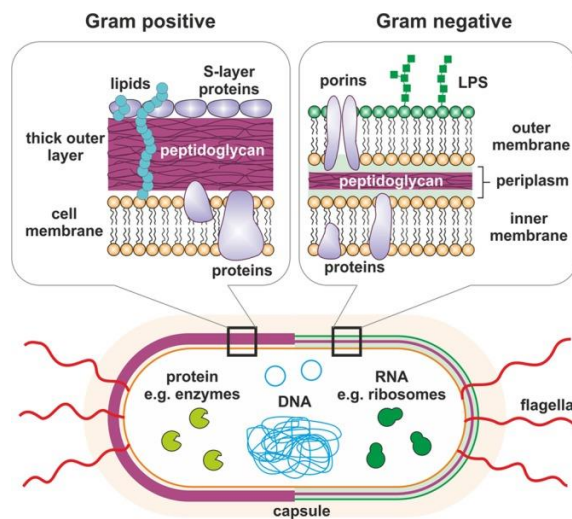
Figure 1.3.1.1: Schematic depiction of the cell walls of Gram-positive and Gram-negative bacteria.[1] Reproduced with permission.

The ability of a bacterium to adhere to a surface is based on physicochemical interactions, such as van der Waals, electrostatic, and acid-base interactions.[11] These

interactions depend on the surface properties of bacteria, which are determined by the chemical composition of the cell wall.[11] Hamadi et al.[11] used X-ray photoelectron spectroscopy (XPS) to determine the chemical composition of the cell wall of *E. coli*, where functional groups could be determined by decomposing XPS peaks. The surface of several strains of *E. coli* were found to be hydrophilic, with C-(C,H), C-(O,N), C=O, OH, and C-O-C functional groups present. Phosphate and carboxyl groups were found to be the main contributors to the surface charge of *E. coli*, which is negative. *E. coli* is therefore more likely to be attracted to positively charged surfaces. The surface properties of bacteria will be important to consider when evaluating the effect of EC-SERS, as the changing electrode potential will result in surface charge changes which in turn influences the adsorption of the bacteria on the surface of the working electrode. As the magnitude of the SERS enhancement is strongly dependent on the distance between the analyte and the surface of the substrate, the signal can be enhanced by drawing the analyte, in this case bacteria, closer to the surface of the SERS substrate.

1.3.2 Bacterial Sensing

Current methods for bacterial identification include culture and colony counting, enzyme-linked immunosorbent assay (ELISA), and polymerase chain reaction (PCR), all of which can take up to one week to yield final results.[2,14] Cultures grown on differential agar media followed by colony counting is a time consuming and laborious process. This method entails pre-enrichment, selective enrichment, biochemical screening and serological confirmation, with interpretation of the results proving to be less than straight forward.[15] Issues can also arise with bacteria not being readily cultivable due to starvation and stress conditions.[15] ELISA, as well as other immunological methods such as enzyme

immunoassay, flow injection immunoassay, immunochromatography strip test, and immunomagnetic separation are all commonly used and based on specific antigen/antibody binding.[15] These tests have poor sensitivity, potential interferences from complex matrices and low affinity of some antibodies to their target bacteria[15]. PCR based methods analyze DNA and have been shown to be more specific, sensitive, and fast compared to other methods.[15] However PCR is expensive, not able to distinguish between living and dead cells, can exhibit high false positive and negative rates, and it is highly susceptible to cross-contamination.[15]

Clearly, these traditional methods for bacterial screening are all lacking in some aspect. Due to these limitations, novel biosensors have been emerging as a possible route for bacterial identification. Nucleic-acid aptamers have recently been attracting interest for their potential use for bacterial detection.[16] Aptamers are RNA or DNA sequences that are made to selectively bind to target molecules, and they can do so with high affinity.[16] Aptamers can bind to their targets in a number of ways, with the most common configuration being the "sandwich" assay, which is a dual site binding method.[16] While aptamer-based biosensors have many applications, they can be tailored specifically for bacterial screening by choosing aptamers specific for the strain of interest. This process uses a method called systematic evolution of ligands by exponential enrichment (SELEX).[12]

Other biosensors that have been explored for pathogen detection include optical, electrochemical, thermometric, piezoelectric, magnetic or micromechanical detectors.[2] Optical biosensors have been the most popular due to their selectivity and sensitivity.[2] Specifically, fluorescence methods, which are based on exciting valence electrons to a

singlet state, and surface plasmon resonance methods, which measure changes in refractive indices, have been growing in popularity.[2] Piezoelectric biosensors are less popular, and are based on the observation of mass change induced resonance frequency changes on a quartz crystal microbalance.[2] Electrochemical biosensors show great promise for pathogen detection, and are based on observed changes in current or voltage due to interactions between the sensor and sample.[2]

Monitoring the presence of pathogenic bacteria is absolutely vital for human health and safety. Because of this, the biosensor industry is rapidly growing with a market that can be categorized into four segments: medical, environmental, food, and military.[17] As a result of the degree to which bacteria can threaten human life, food and medical applications dominate the field of bacterial sensing.[2,17] With the pathogen testing market growing by about 4.5% annually,[17] the increased need for bacterial identification must be met with an efficient screening method to satisfy the increasing need in all segments.
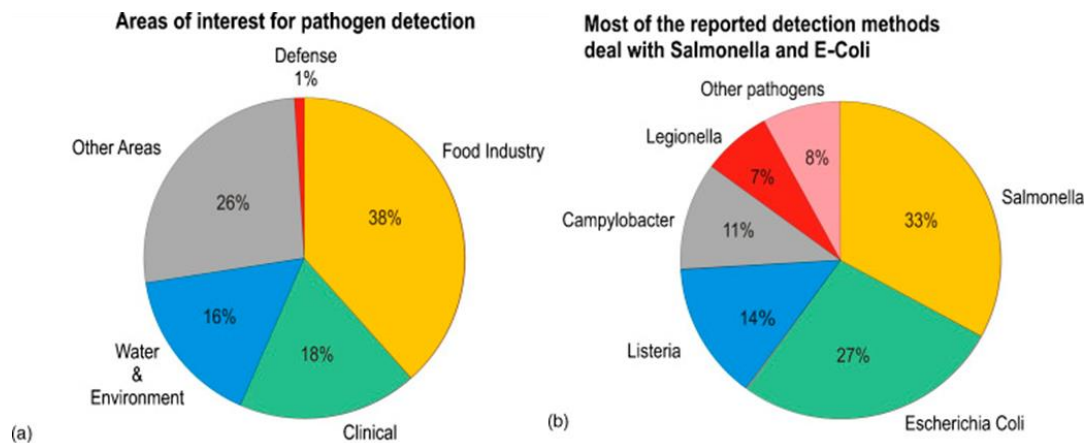
Figure 1.3.2.2: (a) Distribution of the application of pathogen detection by industry based on number of published works, and (b) distribution of micro-organisms of most interest for detection, based on number of published works.[2] Reproduced with permission.

As mentioned, the medical sector is in need of updated bacterial screening technology. Timely identification of bacterial infections can mean the difference between life and death for patients, especially with strains of bacteria becoming resistant to general antibiotics. Improper or inefficient bacterial identification can result in further spread of infectious disease and delayed treatment. Hospitals typically use their own laboratory facilities to identify bacteria, with most samples coming in the form of urine or blood samples.[17] Current detection and identification methods lead to massive back-ups in terms of sample processing with the current technologies affording a massive financial strain for hospitals and health-care systems.[17]

The food industry is greatly affected by bacterial contamination which can lead to widespread illness, death, and recalls that result in significant financial losses and reduced consumer-reputability for businesses. *E. coli* 0157:H7 is one of the major foodborne pathogens that can cause severe illness including diarrhea and acute kidney failure.[14] *Salmonella* and *Listeria* are other major contributors to foodborne illnesses.[18,19] *Salmonella* is one of the main causes of gastrointestinal illnesses, leading to over 1 million illnesses and ~450 deaths per year in the United States.[18] *Listeria* is a major cause of foodborne diseases worldwide; it is particularly dangerous due to its ability to persist in food products for several years.[19] Bacterial screening in the food industry is vital to ensure public safety and to prevent unnecessary spread of foodborne diseases.

Environmental monitoring of bacteria, specifically in water, is essential to ensure that the public has access to safe drinking and recreational water. In urban areas where residents are on public water distribution systems, contaminations can affect many individuals. Water treatment plans typically process water to remove microbial

contaminants before it is transferred to a distribution system.[17] It is here that frequent bacterial screening must take place, in order to ensure there has been no microbial infection of the water supply.[17] Current tests take up to 18 hours which can lead to a delay in identifying a possible threat to public health.[17] Rapid bacteria testing in water distribution systems and treatment plants would help to ensure public safety, as well as decrease extended boil water orders prior to consumption.[17] Exposure to waste water can also result in transmission of infection diseases, so it is important to track faecal contamination of water.[20] With increasing pressure to recycle fresh water, this sector is in need of a cost-effective and rapid bacterial screening platform.

While it accounts for a very small amount of the bacterial detection field, screening of biological warfare agents is of great importance for military applications.[17] In this sector accurate, sensitive, and rapid detection of possibly fatal micro-organisms is vital. The most at-risk citizens for biological warfare agents are overseas military personal, and as such bacterial screening instrumentation must be portable and easy to use. With bioterrorism attacks becoming somewhat more frequent, this sector is specifically in need of a field-based test for biological warfare agents such as *Salmonella, Bacillus anthracis* (anthrax) and *Yersinia pestis* (plague).[21]

Overall, bacterial detection is widely applicable and required by various industries. Despite the importance of bacterial detection, current methods are time consuming, sometimes costly, and require specialized operators. The general consensus is that collectively, the world is in need of a cost-effective, rapid, sensitive, accurate, portable, and easy to use bacterial detection platform. The development of such a technique could improve patient treatment, infectious disease containment, urban water

distribution system safety, the food industry and military personal safety. While many techniques and instruments have been investigated for this application, the field is still lacking a detection platform that encompasses the necessary requirements, including matching or improving upon the sensitivity and selectivity of current methods.

1.3.3 Surface-Enhanced Raman Spectroscopy for Bacterial Sensing

Surface enhanced Raman spectroscopy (SERS) has recently been increasingly explored for bacterial detection, with interest in the field beginning about 15 years ago.[7] SERS is a powerful tool that is an excellent candidate for bacterial screening due to its high sensitivity, relatively low cost, portability, and ability to analyze aqueous samples without spectral interference from water.[22] SERS also generally requires minimal sample preparation and can be used to acquire spectral data in a matter of seconds, making it ideal for PON diagnostics. While many methods of bacterial identification using SERS have been explored, a lack of signal reproducibility remains a major issue.[23,24]

Cho et al. developed a rapid (one hour) method for the detection of *E. coli* 0157:H7 in ground beef using membrane filter-assisted SERS, finding that a low number of bacterial cells could be detected from ground beef homogenates.[14] Najafi et al. presented a study on the detection of *E. coli* 0157 in apple juice, providing a method for liquid food matrices.[25] Gau et al. developed an aptamer-based bacterial detection method, where nanoparticle reduction took place *in situ.* [26] The results of this study showed that the bacteria sample produced signals that could be attributed to adenine. However, without a control study (aptamer with no bacteria), it is impossible to say if the adenine signal was from the bacteria or the aptamer itself. Other studies have also made use of the ability of aptamers and antibodies to capture bacteria for SERS-based bacteria

11

detectors.[27,28] Chen et al. showed that silver nanorod arrays have potential for bacterial screening by using filter membranes as substrates as opposed to typical glass substrates.[29]

Mosier-Boss et al. found a way to eliminate the citrate interference commonly encountered with citrate-reduced silver colloids by allowing bacteria to equilibrate with colloidal silver, which allowed the bacteria to partition through the citrate layer surrounding the nanoparticles.[30] The citrate interference arises from nanoparticles being synthesized with citrate as the reducing and/or capping agent. The citrate on the surface of the nanoparticles can interfere with SERS spectra, as citrate produces a strong SERS spectrum itself. The spectra obtained, while lacking citrate peaks, resembled the SERS spectra of adenine. Zhang et al. showed the potential of 3-dimensional SERS substrates for bacterial detection, these types of substrates increase the number of available SERS hot-spots.[6] Boardman et al. showed SERS spectra of 17 bacterial species, all of which produced similar spectra.[31] The study, however, showed potential for SERS detection of bacteria from blood.

While SERS of bacteria has clearly become a widely explored method, a biological basis for the observed signals has not been established, which limits the expansion and applicability of the field.[7] There has been much controversy in the field as to what the SERS signals of bacteria can be attributed to. Premasiri et al. have shown that the observed bacterial SERS signals are decidedly not due to structural bacterial cell wall features, but instead represent linear combinations of the SERS spectra of adenine, hypoxanthine, xanthine, guanine, uric acid, and AMP, which are purines that exist in the extracellular metabolome surrounding bacteria cells.[7] These purines are the products of nucleotide degradation, a process which results when the bacteria are experiencing stress

or starvation conditions. Guanosine was recently determined to be another contributor to the SERS spectra of bacteria. The attribution of all bacterial SERS spectra to the same handful of molecules makes strain differentiation extremely challenging, as it cannot at present be done based on the presence or absence of peaks that would be specific to the unique cell wall components of different bacteria.

Since bacterial strain differentiation is key for implementing SERS as a widespread method for bacterial screening, it was necessary to find a means to achieve this despite the similarities between bacterial SERS spectra. To address this need, Patel et al. developed a bacterial barcoding method, which involves the generation of barcodes for separate strains of bacteria based on the second derivative SERS spectrum.[8] To do this, a minimum value of about 10% of the maximum second-derivative value is used as a threshold for zero to discriminate against residual noise components, which is followed by assignments of 1 or 0 to the intensities. These assignments are made by assigning +1 for positive second derivatives, representing upward curvature, where positive values are defined to be those greater than the selected zero threshold. A value of 0 is then assigned to all negative second derivative intensity values, which signifies downward curvature, where negative values are defined to be those less than the selected zero threshold. This bacterial barcode can then be used as an input for principal component analysis (PCA), which is then used to construct dendrograms from hierarchical cluster analysis (HCA) calculations. Patel et al.[8] were able to show that by employing this barcoding method, maximum bacterial species differentiation could be achieved, as compared to using the normal SERS spectra or the first or second derivative spectra as inputs for PCA. Before the bacterial barcoding method was developed, cluster analysis was shown to be one of

the only viable methods for SERS-based bacterial species discrimination.[32] While bacterial barcoding has proven to be useful for differentiating between bacterial strains,[8,33] it would be ideal to be able to do so based on spectral differences detected by a database of known bacterial strains. The use of mathematically rigourous processes can slow down interpretation of results, and thus patient treatment if it were to be employed in a hospital setting for bacterial testing.

One important aspect to consider with SERS detection of bacteria when using a silver coated substrate is the antibacterial properties of silver. There has been evidence to show that silver nanoparticles can inherit the antimicrobial abilities of ionic silver, although the exact toxicity mechanism is still not known.[24] Studies have shown that the toxicity depends on factors including impurities, nanoparticle size, shape, and surface properties.[34] Badawy et al. further investigated the contributors to nanoparticle toxicity with *Bacillus* bacteria, showing that impurities such as ionic silver, and various reducing and capping agents can contribute to the nanoparticle toxicity, but not enough to suggest significant toxicological impacts.[34] This study also demonstrated that particle size was not the dominant contributing factor to nanoparticle toxicity. This study concluded that silver nanoparticles can be toxic to bacteria, and the main contributor to the toxicity is the native surface charge of the silver nanoparticles.

The importance of the toxic effects of silver nanoparticles on bacteria for SERS sensing has not been agreed upon. Zeiri et al. suggested the basic biochemical makeup of bacteria is retained even if the bacteria are dead.[22] However, a study on the SERS discrimination between live and dead bacteria by Zhou et al. disproved this statement, showing that it does matter if the bacteria are dead or alive.[35] The authors showed that

14

live bacteria adsorbed onto silver nanoparticles (AgNPs) produced strong SERS signals, and the SERS signal decreased with increasing amounts of dead bacteria. This study suggests that it may be important to ensure that bacteria are still living to obtain high quality SERS spectra.

The possible interference of cell growth media on observed SERS spectra of bacteria was speculated by Marotta and Bottomley to be significant. These authors claimed that the SERS spectra reported in work by others were actually from the cell growth media not being completely removed from the cultured bacterial cell samples.[36] This hypothesis was based on the resemblance between the SERS spectra of bacteria and of several cell growth media, the appearance of a SERS spectrum only after dilution, the similarity between SERS spectra of Gram-positive and Gram-negative bacteria and the spatial distributions of the bacteria-like spectrum on the SERS substrate.[36] Premasiri et al.[37] were able to disprove this theory using multivariate data analysis to show that the same bacterial species grown in different media show the same SERS spectra. This uncertainty could be removed by carrying out a control study with no bacteria present, and will therefore be done in this thesis work to ensure no interference from cell growth media.

In summary, it is evident that there is a significant amount of confusion in the field, with conflicting results hindering the forward movement of this method for bacterial detection. At present, there is no current satisfactory method that makes use of SERS for bacterial identification despite its immense promise to provide a fast and cheap method for such an application. This thesis work aims to improve upon the ability of

normal SERS for bacterial detection, ensuring reproducibility and carrying our proper control studies to eliminate the confusion that has been associated with past studies.

1.4 Theory

1.4.1 Raman Spectroscopy

Spectroscopy, the study of the interaction of matter with incident electromagnetic radiation, is a useful technique for quantitative and qualitative analysis of samples. The spectroscopic technique of Raman spectroscopy was first introduced in 1928 by Raman and Krishnan.[38] Raman spectroscopy is scattering technique which is based on the interaction of incident radiation with vibrating molecules causing inelastic scattering. This occurs when a monochromatic (single wavelength) laser source illuminates a sample, causing light to scatter. The inelastic portion of the scattered light is the light that is scattered at a different frequency from that of the incident light.[3] However, the majority of the scattered light that arises is equal in frequency to the incident light, which is called Rayleigh scattering (elastic scattering).[3] When a photon is excited from the ground state and relaxes down to a higher energy state and the frequency of relaxation is less than the frequency of the incident light, Stokes lines appear on a Raman spectrum.[3] When a photon is excited from a state higher than the ground state and the frequency of relaxation is more than the frequency of the incident light, anti-Stokes lines appear on a Raman spectrum.[3] Figure 1.4.1.1 shows a schematic representation of the Rayleigh, Stokes, and anti-Stokes scattering of light. Stokes lines are more intense than anti-Stokes lines, as the intensity of Stokes lines is proportional to the number of molecules in the ground state, and the intensity of anti-Stokes lines is proportional to the number of molecules in an excited state, which is less populated. Because of the increased intensity of Stokes lines,

they are typically the ones chosen to be monitored in conventional Raman spectroscopy.[3] Raman activity is based on a change in polarizability of a molecule during molecular vibration, which is probed by the incident radiation.[3] Raman spectroscopy is an extremely valuable technique, as it provides a molecular fingerprint for an analyte of interest.[39] Raman spectroscopy can be widely applicable due to its non-destructive nature, however the small amount of Raman scattering that occurs causes this technique to be inherently weak.[39]
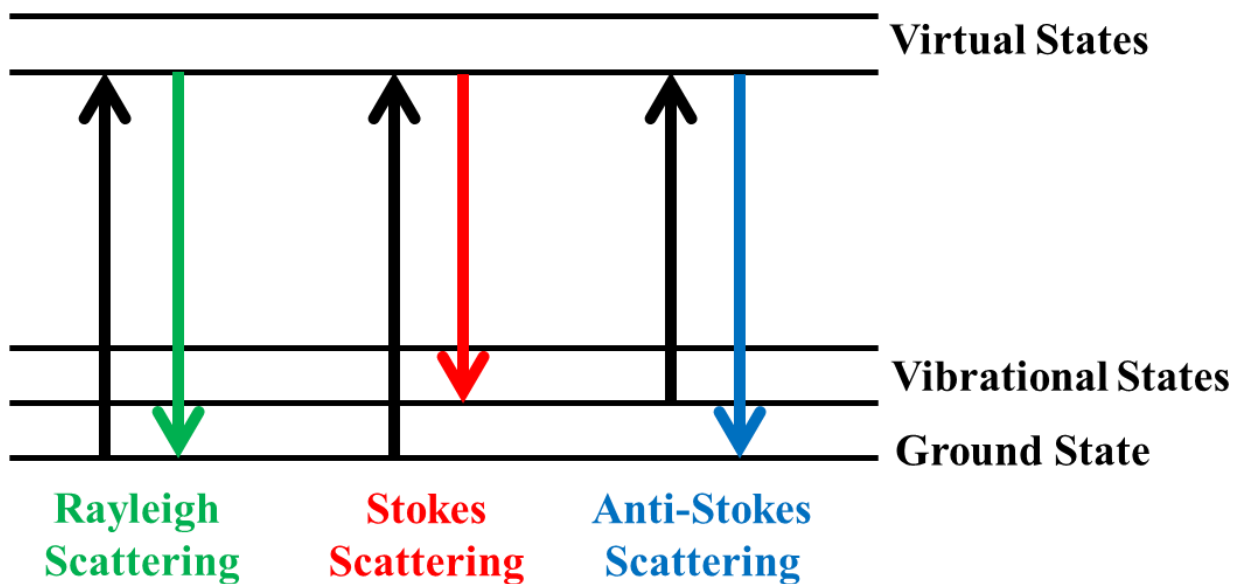
Figure 1.4.1.1: Figure showing the different light scattering modes: Rayleigh, Stokes, and anti-Stokes scattering.

1.4.2 Surface-Enhanced Raman Spectroscopy

As Raman spectroscopy provides useful information, yet is limited by the lack of efficient Raman scattering, surface-enhanced Raman spectroscopy (SERS) was developed to overcome the inherent weakness associated with normal Raman spectroscopy. To

17

enhance the signal produced from normal Raman spectroscopy, SERS was developed by having the target molecule on or very near a roughened noble-metal substrate.[40] SERS makes use of the localized surface plasmon resonance (LSPR) of certain nanoscale metals such as silver, gold, and copper.[40] When the LSPR of these metal substrates is excited by incident radiation, it causes the generation of strong electromagnetic fields.[41] Figure 1.4.2.1 shows a schematic representation of the LSPR created by the interaction of incident light and the free electrons of a metal nanosphere. This strong electromagnetic field causes an increase in the induced dipole of the analyte molecule, resulting in more inelastic scattering. This is the electromagnetic enhancement of SERS, which exhibits theoretical enhancement factors of up to 10 orders of magnitude.[42]
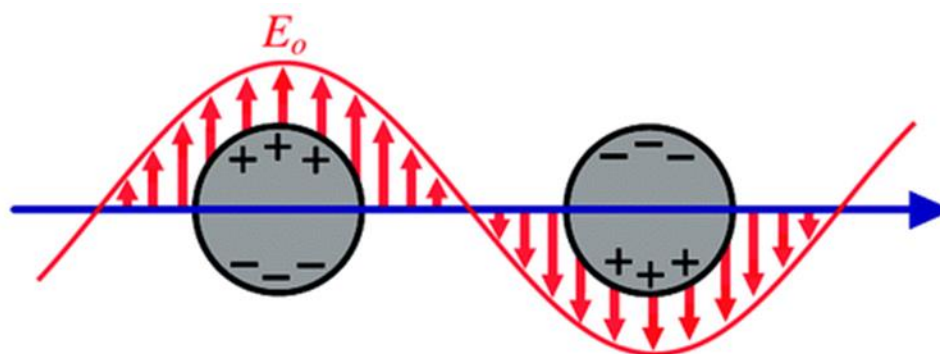
Figure 1.4.2.1: Schematic depiction of the interaction of the collective oscillation between the electric field of the incident light and the free electrons at the surface of the nanosphere.[41] Reproduced with permission

The other contributor to the total SERS enhancement is the chemical enhancement, which involves charge transfer mechanisms when the excitation wavelength is resonant with the metal-molecule charge transfer electronic states.[42]

Theoretical chemical enhancement factors of up to 10^3 have been calculated.[42] The total SERS enhancement is thus a product of the electromagnetic and chemical enhancement factors, which may extend to 10^{10}-10^{11} for highly optimized surfaces.[42] Work by Kneipp and many others suggest that the electromagnetic enhancement mechanism plays a more significant role than the chemical enhancement mechanism in SERS.[43]

As mentioned, SERS usually employs substrates fashioned from gold, silver, or copper, where copper is the least popular choice due to its lack of air stability and difficulty in synthesizing stable nanostructures,[41] although it is the most earth abundant of the three. For a material to be plasmonic, it must support the electromagnetic enhancement by having a complex dielectric function (ε) with a negative real component (ε_r) and a small, positive imaginary component (ε_i).[41] This is based on Mie theory and the equation for calculating the extinction cross section shown below, as the value for the extinction cross section becomes larger when the dielectric function is as described above.[41]

$$C_{\text{ext}} = \frac{24\pi^2 R^3 \varepsilon_m{}^{3/2}}{\lambda} \left(\frac{\varepsilon_i}{(\varepsilon_r + 2\varepsilon_m)^2 + \varepsilon_i{}^2} \right)$$

Figure 1.4.2.2 shows a plot of the real components for ε (A), and the imaginary components for ε (B) for silver, gold, and silicon as a function of wavelength. This figure demonstrates why silver and gold are ideal for SERS, as they have negative real components for ε and small, positive (near zero) imaginary components for ε.[41] The surface plasmon strength of the metal, or the damping, is described using the quality factor, Q, where large quality factors indicate good plasmonic performance. Silver has the

largest quality factor across most of the UV-Vis-NIR spectrum from 300 to 1200 nm, which explains its excellent performance for SERS in this thesis work.
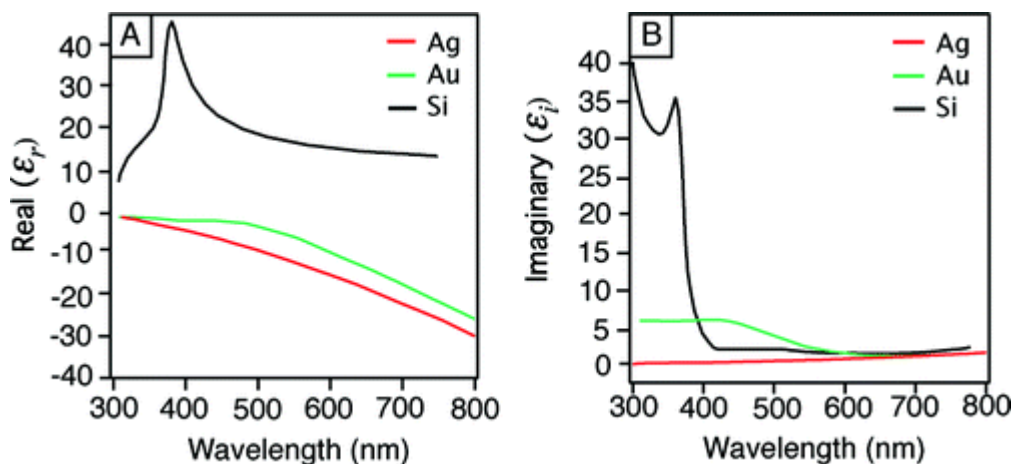
Figure 1.4.2.2: Plot of the real components for ε (A), and the imaginary components for ε (B) for silver, gold, and silicon as a function of wavelength.[41] Reproduced with permission.

SERS is a very sensitive technique, with the detection of a single molecule having been reported.[40] SERS is an excellent candidate for the detection of biological molecules due to its ability to detect multiple analytes at once due to its well-resolved bands, and its ability to be used for analysis of analytes in aqueous solutions.[40] SERS sensing can also be done very rapidly, and is therefore ideal for PON screening. For these reasons, SERS has attracted great attention for bacterial sensing, which has led to the recent development of the field of SERS-based bacterial screening.

1.4.3 Electrochemistry

Electrochemistry takes place on surfaces, where chemical changes can be attributed to charge separations.[44] Electrochemistry is vastly applicable, with uses including industrial electrolysis, electroplating, batteries, fuel cells, and biosensors.[44]

Potentiostatic measurements are one of the main types of experiments in electrochemistry, where the electrochemical cell consists of at least two electrodes and a conductive solution.[45] Potentiostatic techniques study the charge transfer process at the interface of the electrode and the solution where the current of an electrode potential derived electron-transfer is measured.[45] Potentiostatic techniques also measure chemical species that can be made to reduce or oxidize.[45] These techniques are highly sensitive and selective, portable and cost-effective.[45]

When in contact with a polar medium, surfaces develop a surface charge, attracting ions of opposite charge to the surface.[45] This forms the electrical double layer, which is schematically represented in Figure 1.4.3.1 as described by the Grahame model. The two layers are termed the compact and the diffuse layers, where the compact layer contains both Helmoltz planes (inner and outer).[45] The inner Helmoltz plane (IHP) is the layer closest to the surface and contains specifically adsorbed ions, which can be adsorbed via covalent or van der Waals forces, while the outer Helmoltz plane (OHP) is an imaginary plane passing through the center of solvated and non-specifically adsorbed ions.[46] The diffuse layer is a gradient of charge accumulation extending from the outer Helmoltz plane to the bulk solution.[46]
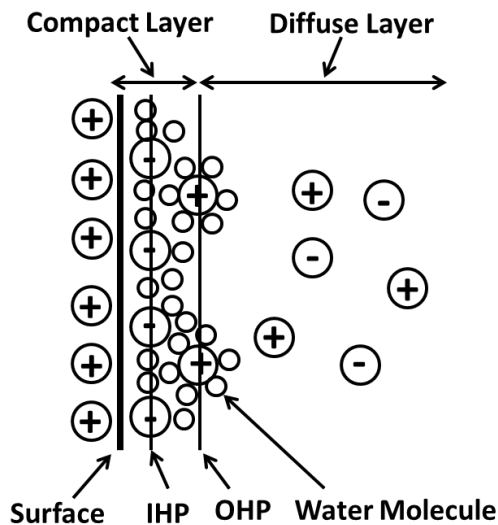
Figure 1.4.3.1: Schematic depiction of the electrical double layer (Grahame model).

Electrochemical cells containing three electrodes are commonly used for experiments where the electrode potential is carefully controlled.[45] Of the electrodes, one is termed the indicator or working electrode (WE), which is where the electrochemical process of interest takes place.[45] The electrode of constant potential, independent of the solution properties is termed the reference electrode (RE), with the silver-silver chloride (Ag/AgCl) RE being one of the most common.[45] Counter electrodes (CE) allow one to measure the potential of the working electrode while passing current.[45] The electrolyte used is chosen based on solubility of the analyte, electrical conductivity, and electrochemical stability.[45] In potential-controlled experiments, electrolytes are usually in the concentration range of 0.1-1.0 M, and are meant to maintain high ionic strength, decrease resistance of the solution, and eliminate electromigration effects.[45] Oxygen can interfere with electrochemical measurements, and so dissolved oxygen is usually removed from electrolyte solution by purging with an inert gas.[45] Electrochemical cells can be Galvanic or electrolytic, where Galvanic cells are spontaneously functioning and

electrolytic cells require electrical energy to be supplied from an external voltage source.[44]

1.4.4 Electrochemical Surface-Enhanced Raman Spectroscopy

As SERS sensing is usually done using noble metal substrates, it is natural to combine this technique with electrochemistry.[47] This spectroelectrochemical technique is termed electrochemical SERS, or EC-SERS, which can be used as a sensitive, simple, cost-effective, and portable detection platform.[48] Applying an electric potential to the surface of a SERS substrate *in situ* has been shown to increase the peak intensity of the studied analyte, therefore improving upon the already high sensitivity of SERS.[9,10] EC-SERS measures the Raman spectra of the molecules adsorbed to the surface of an electrode, and monitors changes as a result of applied voltage or current.[49] These changes can include complete adsorption or desorption of molecules, or electrochemical conversion into other molecular species.[49] Other observed changes may include molecular reorientation of the analyte or rearrangement of the electrical double layer.[49] EC-SERS has been shown to be a sensitive method for the detection of biological molecules such as DNA, nucleotides, DNA aptamers[9], and drug metabolites.[10]

As previously mentioned, silver nanoparticles can exhibit toxic effects towards bacteria which may or may not affect the SERS spectra of bacteria. The study by Badawy et al.[34] also investigated the surface charge-dependent toxicity of silver nanoparticles. They found that the carboxyl, phosphate, and amino groups on the cellular membrane of the Gram-positive bacteria provide the organisms with a negative charge, meaning there is a high degree of repulsion between negatively charged silver surfaces and bacteria,

forming a protective electrostatic barrier. This barrier also limits the interaction between the particles and nanoparticles, which could decrease the SERS enhancement. The authors noted that only *Bacillus* bacteria were studied, and other species could have different degrees of resistance towards the charge induced physical interactions. The findings of this study are important to consider for EC-SERS of bacteria, as changing the surface charge of the nanoparticles can affect their toxic behaviour towards bacteria.

Chapter 2: Results and Discussion

2.1 Substrate Preparation

As this project represents the first time EC-SERS is used for bacterial screening, it was first vital to select an appropriate metal substrate and laser line. The options for EC-SERS measurements for this study included an AgNP coated substrate using the 780 nm or 532 nm laser line, or a gold nanoparticle (AuNP) coated substrate using the 780 nm laser line. Carbon screen printed electrodes (SPEs) were used as the substrate, with the nanoparticle coating drop-cast onto the working electrode (WE). Figure 2.1.1 shows a SPE with the counter electrode (CE), working electrode (WE), and Ag/AgCl reference electrode (RE) labelled. These electrodes only cost several dollars to purchase and are disposable, making them an ideal candidate for cost-effective substrates. All three substrate and laser combinations were used to characterize all seven nucleotide breakdown products to determine the optimal measurement conditions to move forward with for bacterial detection. Using a SPE modified with AgNPs with the 780 nm laser line gave the best results, which is why only those results are shown in this thesis, although the results for all other substrate conditions can be found in the appendix (Figures A2-15). The silver nanoparticles used for this study were mostly spherical and approximately 20 nm in diameter.[9]

Figure 2.1.1: Labeled SPE, which was used as the EC-SERS substrate in this thesis work.

It was expected that silver nanoparticles would work better than gold nanoparticles, as they have been shown to scatter light better than gold nanoparticles of the same size due to their optical properties.[50] The 780 nm laser line was beneficial over the 532 nm laser line as it is less energetic, and therefore less likely to damage biological samples or cause photo-degradation. Additionally, less interfering fluorescence is observed when a less energetic laser is used.

All substrates used underwent a chloride displacement treatment by immersing the substrate in 0.5 M KCl for 30 minutes, followed by a 30 second rinse with water. This process was done to remove citrate from the surface of the nanoparticles, as citrate was used as the capping agent in the nanoparticle synthesis. The chloride displacement treatment works by displacing the surface adsorbed citrate ion with Cl⁻, as it has a strong specific adsorption on Ag, which is represented schematically in Figure 2.1.2.[51] Citrate is Raman active, it produces strong peaks at ~935 and ~1404 cm^{-1} which are assigned to ν(C–COO) and ν_s(COO) vibrations, respectively, as well as peaks at 810 and 840 cm^{-1} from ν(CCCC-O) vibrations, and a peak at 1033 cm^{-1} from ν(C-O) vibrations.[51] Additionally, citrate is negatively charged and can therefore cause electrostatic repulsion of analytes. Citrate therefore has the ability to significantly interfere with the adhesion of bacteria to the surface of the electrode, as well as detection. Chloride, however, only produces one strong peak at 240 cm^{-1} which is due to ν(Ag-Cl) vibrations, and therefore interferes less with the EC-SERS spectrum.[51]
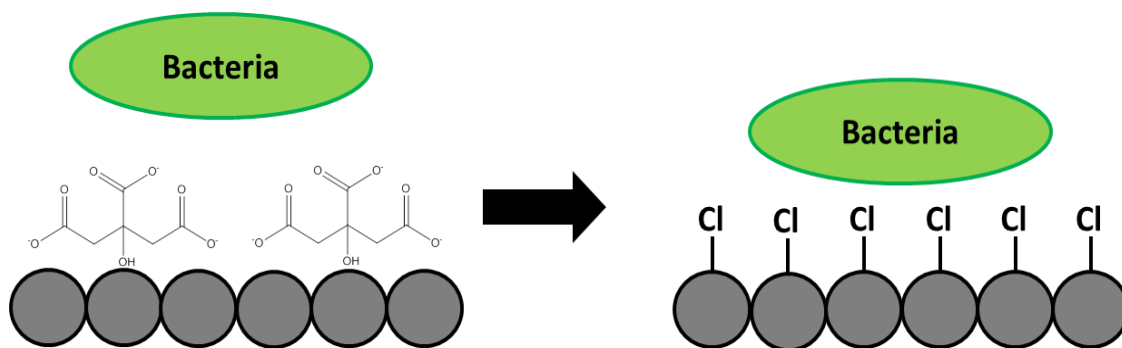
Figure 2.1.2: Schematic representation of chloride displacement treatment.

2.2 EC-SERS of Nucleotide Breakdown Products

As the SERS spectra for bacteria have been shown to be attributed to the nucleotide breakdown products adenine, hypoxanthine, xanthine, guanine, uric acid, AMP and guanosine, it was vital to first establish reference EC-SERS data for all seven molecules in order to determine if EC-SERS spectra obtained for bacteria could be attributed to one or a combination of these molecules. The molecular structures of each molecule are shown in Figure 2.2.1. For each molecule, 5.0 µL of a 5.0 mM aqueous solution was drop coated onto the working electrode surface of a KCl-treated screen printed electrode and allowed to dry. The screen printed electrode (the EC-SERS substrate) was then placed into the glass electrochemical cell and used to acquire a normal SERS spectrum, termed the "in air" spectrum. pH 7.4 phosphate buffer, the supporting electrolyte, was then added to the cell (enough to fully cover the working electrode) after being purged of oxygen using argon gas, and the cell was connected to the potentiostat. A control study to ensure there would be no spectral interference from the phosphate buffer electrolyte can found in the Appendix (Figure A1). Before the application of a potential, a spectrum was obtained at open circuit potential (OCP), which is termed the OCP cathodic spectrum. A spectrum was always recorded with an applied potential of 0 V vs Ag/AgCl.

The applied potential was then progressively stepped in the negative (cathodic) direction in increments of 0.1 V until a final potential of -1.0 V was reached (note the potential for gold EC-SERS substrates was varied between 0.4 V and -0.6 V). The potential was then stepped back in the positive (anodic) direction in increments of 0.1 V from -1.0 V to 0.0 V.
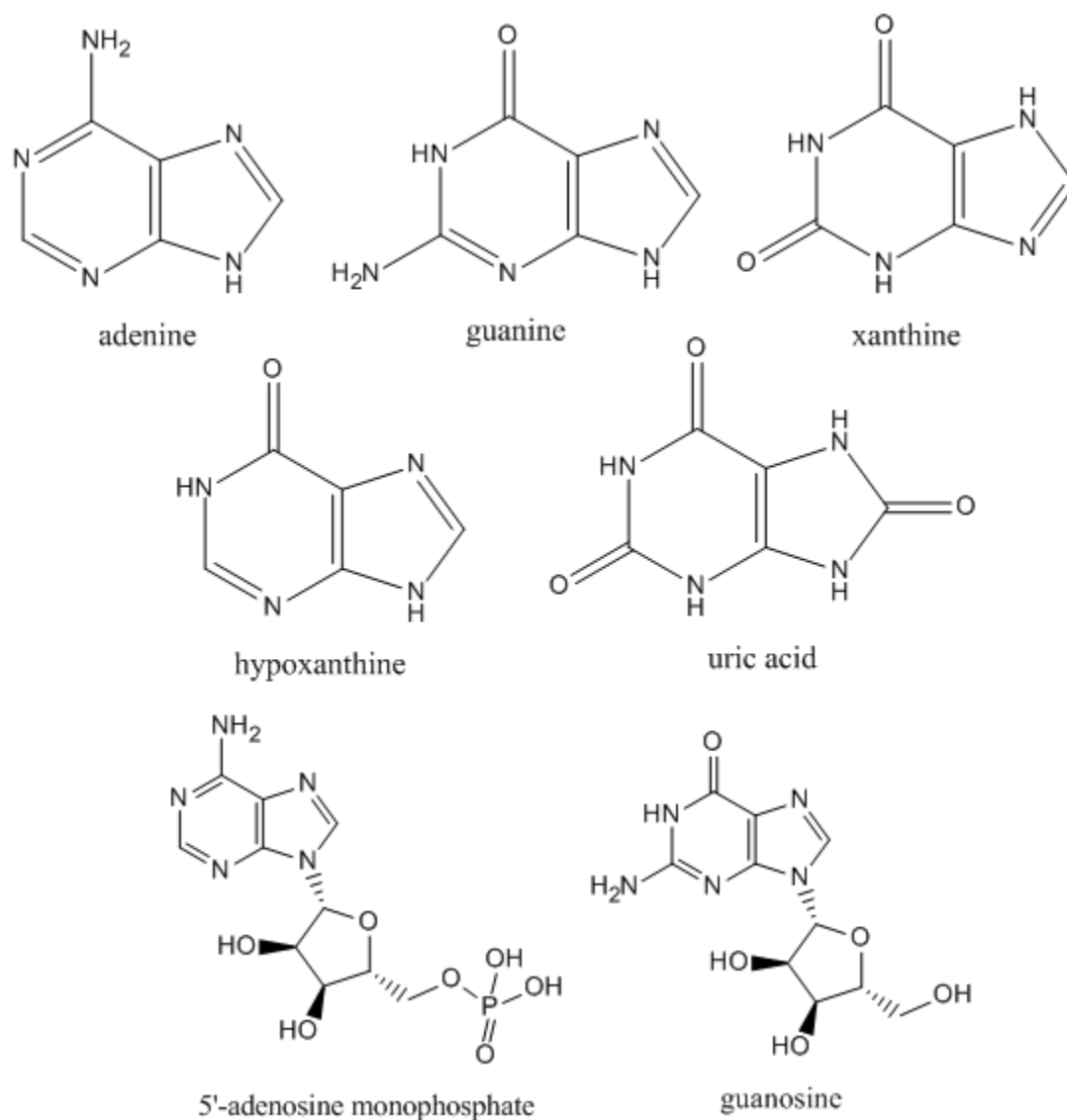
Figure 2.2.1: Structures of the seven nucleotide breakdown molecules: adenine, guanine, xanthine, hypoxanthine, uric acid, AMP, and guanosine.

Figure 2.2.2 A shows the cathodic progression of adenine on the AgNP modified SPE using the 780 nm laser line to demonstrate the effect of applied potential on the SERS spectrum, with an overlay of the EC-SERS spectrum from the OCP (cathodic) spectrum at the bottom, to the -1.0 V spectra at the top. This shows how the spectral intensity and quality improves greatly with the application of potential. Figure 2.2.2 B shows the comparison of the in air, OCP cathodic, optimized negative potential, and OCP anodic spectra for adenine on silver using the 780 nm laser line. The EC-SERS spectrum at -1.0 V is a significant improvement over the in air spectrum. The in air spectrum is obtained before EC-SERS is commenced, and thus represents the corresponding normal SERS experiment, as the in air spectrum is all that could be obtained without employing an applied potential. As bacterial spectra can be attributed to adenine and the other breakdown molecules, this observation shows that EC-SERS has the potential to improve upon the normal SERS spectra of bacteria significantly.

Figure 2.2.2: (A) Cathodic progression of the SERS spectra and (B) EC-SERS comparison for adenine on silver using an excitation wavelength of 780 nm with a laser power of 80 mW for an acquisition time of 30 seconds.

Figures 2.2.3 – 2.2.8 show the cathodic progressions and EC-SERS comparisons for the other 6 nucleotide breakdown products. Figure 2.2.3 A shows the cathodic progression of the EC-SERS signal for guanine on a silver substrate using the 780 nm laser line, showing that the optimized negative EC-SERS spectrum is at -1.0 V, as it was with adenine. Interestingly, Figure 2.2.3 B showing an EC-SERS comparison for guanine shows that the SERS signal did not deteriorate going from -1.0 V to OCP anodic. Figure 2.2.4 shows the same spectra for xanthine, where again the SERS signal was optimized at -1.0 V. Figure 2.2.5 shows the same spectra for hypoxanthine, where the SERS signal is again optimized at -1.0 V. The cathodic progression of the hypoxanthine SERS spectrum (Figure 2.2.5 A) shows peaks at 720 and 735 cm^{-1} at OCP cathodic, however as more negative potentials are applied, only the 720 cm^{-1} peak is visible, which is indicative of the enol tautomer of hypoxanthine.[52] The peak at 735 cm^{-1} can be attributed to the keto tautomer of hypoxanthine, demonstrating that both the keto and enol forms are present at OCP, but a negative applied potential causes only the enol form to dominate in the SERS spectrum.[52]

Figure 2.2.6 shows the cathodic progression and the EC-SERS comparison for AMP, where the SERS spectrum is optimized at 0.0 V. This suggests that a negative potential does not enhance the SERS performance of AMP, so it is likely that negative potentials push AMP further from the surface of the WE of the SPE, thus decreasing the SERS enhancement. The same spectral comparisons for uric acid, Figure 2.2.7, show that the optimized negative EC-SERS spectrum for uric acid is at -0.3 V. Figure 2.2.8 contains the same spectral comparisons for guanosine, where the optimized negative EC-SERS spectrum is at -0.8 V. All data for the seven molecules and the mixture of all seven on

silver using the 532 nm laser line and on gold with the 780 nm laser line can be found in the Appendix (Figures A2-A15).
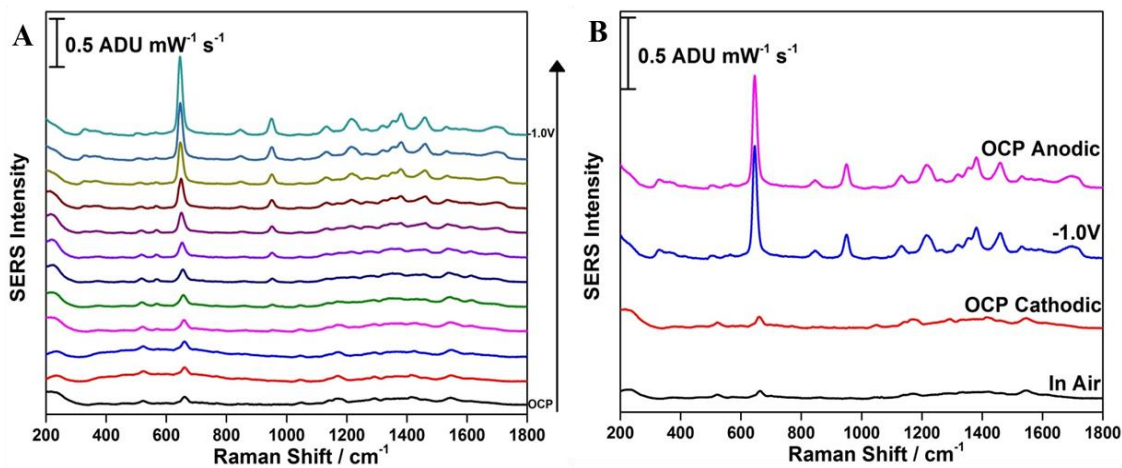
Figure 2.2.3: (A) Cathodic progression of the SERS spectra and (B) EC-SERS comparison for guanine on silver using an excitation wavelength of 780 nm with a laser power of 80 mW for an acquisition time of 30 seconds.
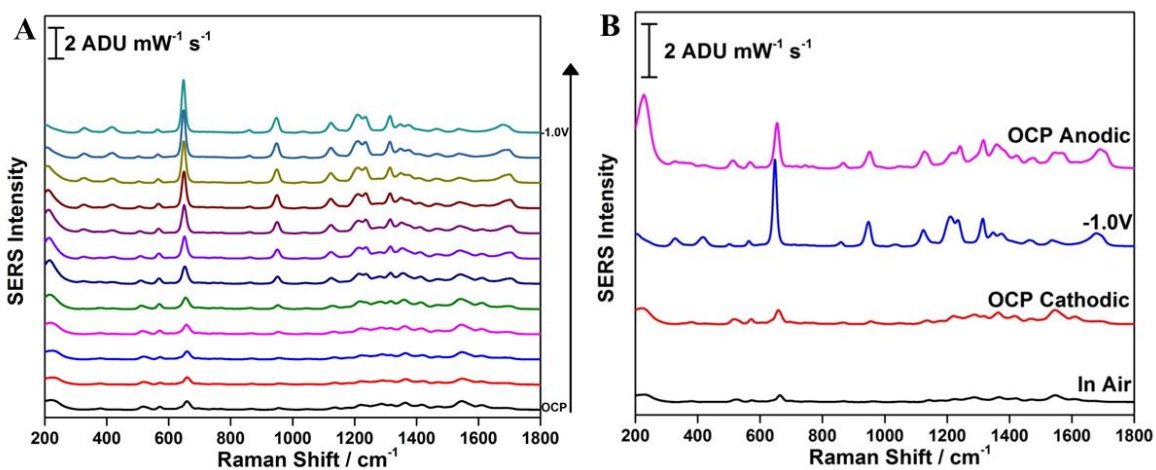
Figure 2.2.4: (A) Cathodic progression of the SERS spectra and (B) EC-SERS comparison for xanthine on silver using an excitation wavelength of 780 nm with a laser power of 80 mW for an acquisition time of 30 seconds.
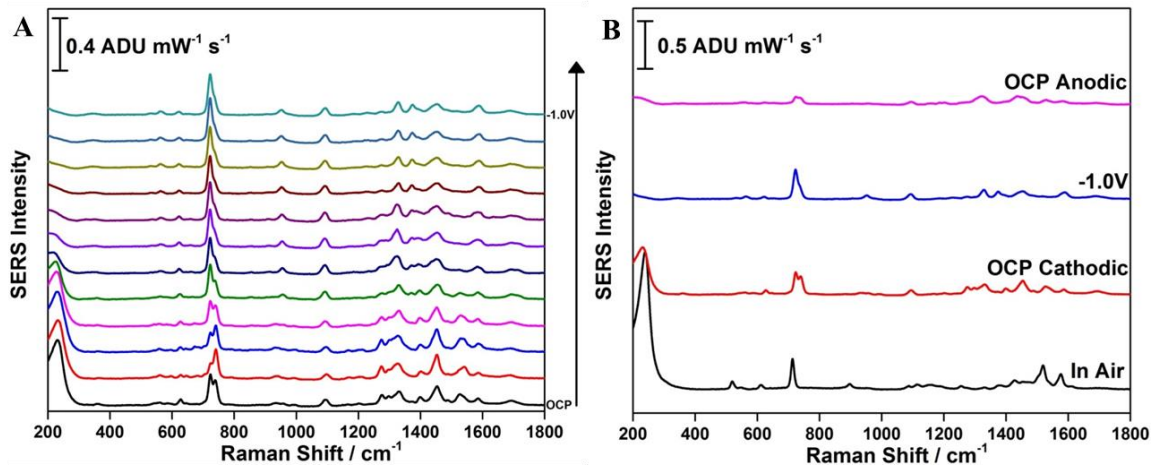
Figure 2.2.5: (A) Cathodic progression of the SERS spectra and (B) EC-SERS comparison for hypoxanthine on silver using an excitation wavelength of 780 nm with a laser power of 80 mW for an acquisition time of 30 seconds.
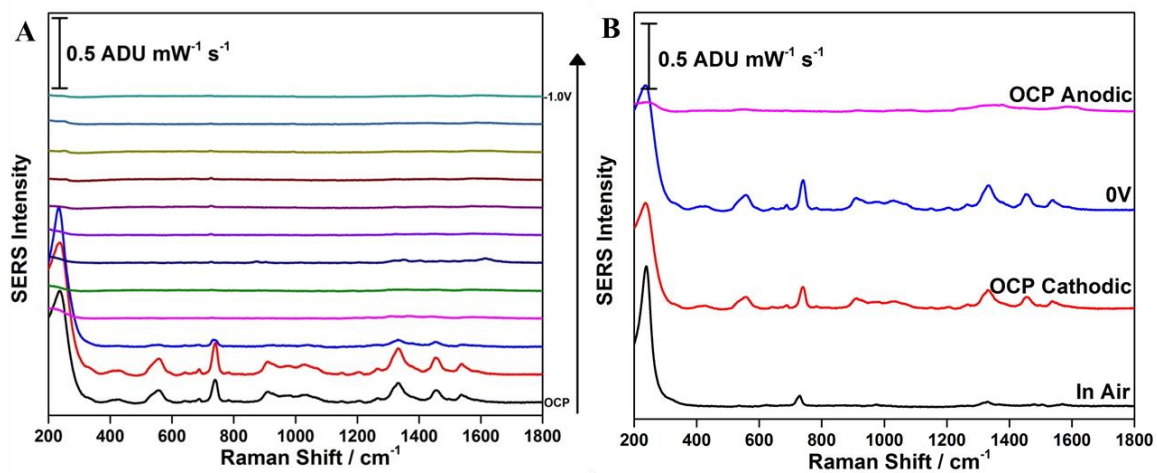
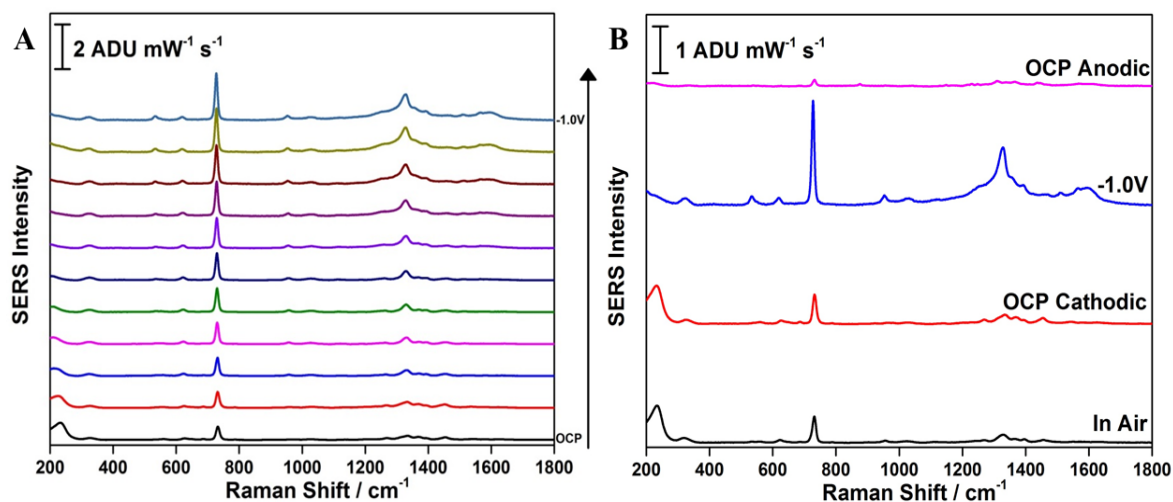**Figure 2.2.6:** (A) Cathodic progression of the SERS spectra and (B) EC-SERS comparison for AMP on silver using an excitation wavelength of 780 nm with a laser power of 80 mW for an acquisition time of 30 seconds.
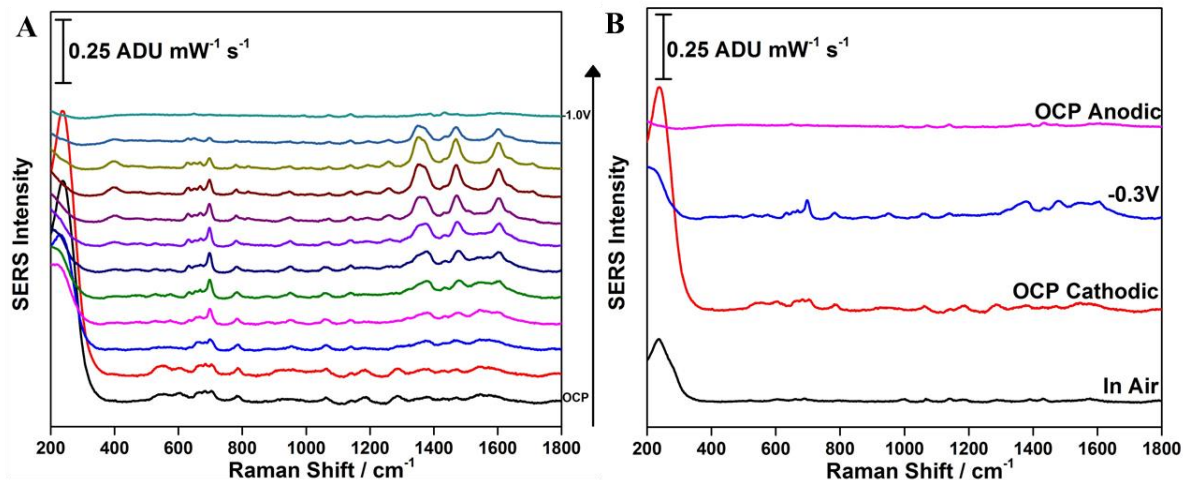
Figure 2.2.7: (A) Cathodic progression of the SERS spectra and (B) EC-SERS comparison for uric acid on silver using an excitation wavelength of 780 nm with a laser power of 80 mW for an acquisition time of 30 seconds.
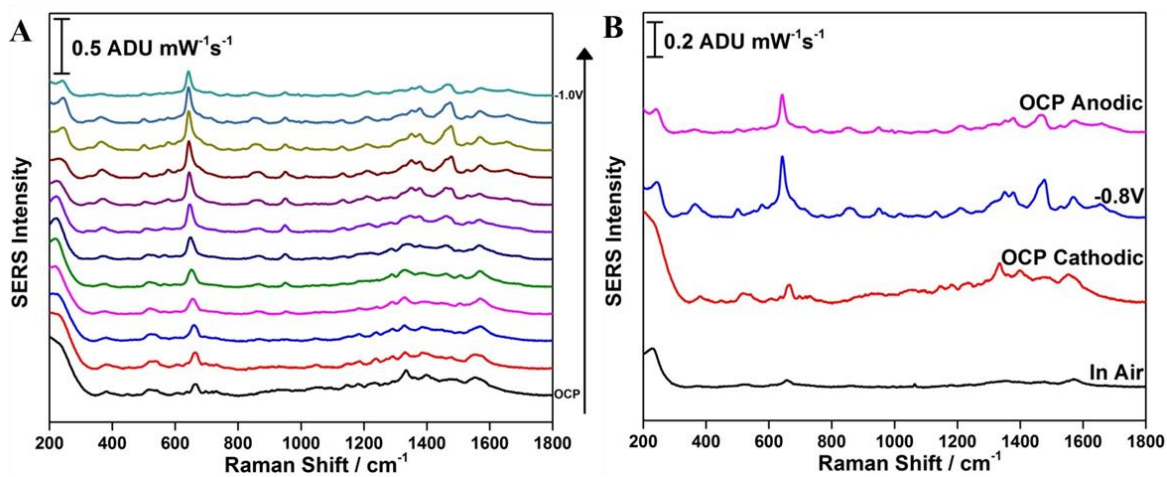
Figure 2.2.8: (A) Cathodic progression of the SERS spectra and (B) EC-SERS comparison for guanosine on silver using an excitation wavelength of 780 nm with a laser power of 80 mW for an acquisition time of 30 seconds.

For ease of viewing, Figure 2.2.9 shows the best SERS spectra for each of the seven nucleotide breakdown products at various negative potentials silver EC-SERS substrates, as well as the spectrum obtained for a mixture of all seven of the products. The same study as was done for the individual nucleotide breakdown products was done for an equal mixture of all seven breakdown products in order to get a better idea of what

33

molecules would dominate the SERS spectra when all were present in a mixture. Figure 2.2.10 A shows the cathodic progression for the mixture on silver using the 780 nm laser, and Figure 2.2.10 B shows the EC-SERS comparison. The -1.0 V spectrum from Figure 2.2.10 B (the optimized EC-SERS spectrum for a mixture of all seven breakdown products) was run through spectral database containing the optimized EC-SERS spectra for all individual breakdown products to determine the relative contributions of the individual products on the spectra of the mixture. For this database, Thermo Scientific™ OMNIC™ Specta Software was used, creating a database of spectral data through a unique combination of spectral identification tools, interpretation algorithms, and scientific documentation. It was found that adenine was the main contributor, with an 88% match to the spectrum of the mixture. Hypoxanthine, guanine, xanthine, guanosine, AMP, and uric acid matched 75%, 44%, 41%, 38%, 15%, and 9% respectively with the spectrum of the mixture. This indicates that when all breakdown products are combined, the spectral peaks of adenine and hypoxanthine dominate the spectrum. This could suggest that adenine and hypoxanthine will be a main contributor to the EC-SERS spectra of bacteria. The peak assignments for all major peaks in the seven nucleotide breakdown products can be found in the Appendix (Tables A1-A7) along with the labeled optimized negative EC-SERS spectra (Figures A16-A22).
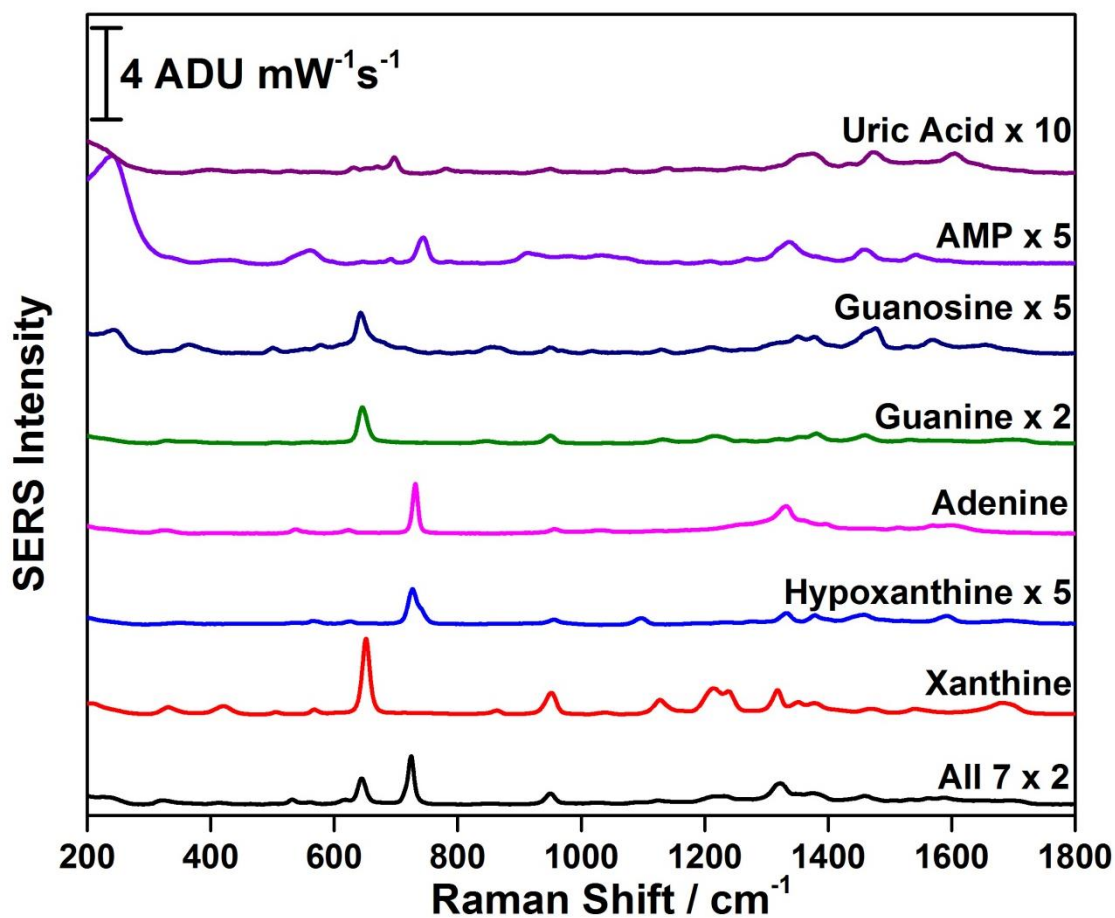
Figure 2.2.9: Combination of EC-SERS spectra of all seven nucleotide breakdown products, including a mixture of all seven on silver using the 780 nm laser line. The spectra included are the optimized spectra from various negative potentials and have been scaled to be similar in intensity for comparison purposes (scaling factor indicated in figure). All spectra were collected with a laser power of 80 mW for an acquisition time of 30 seconds.
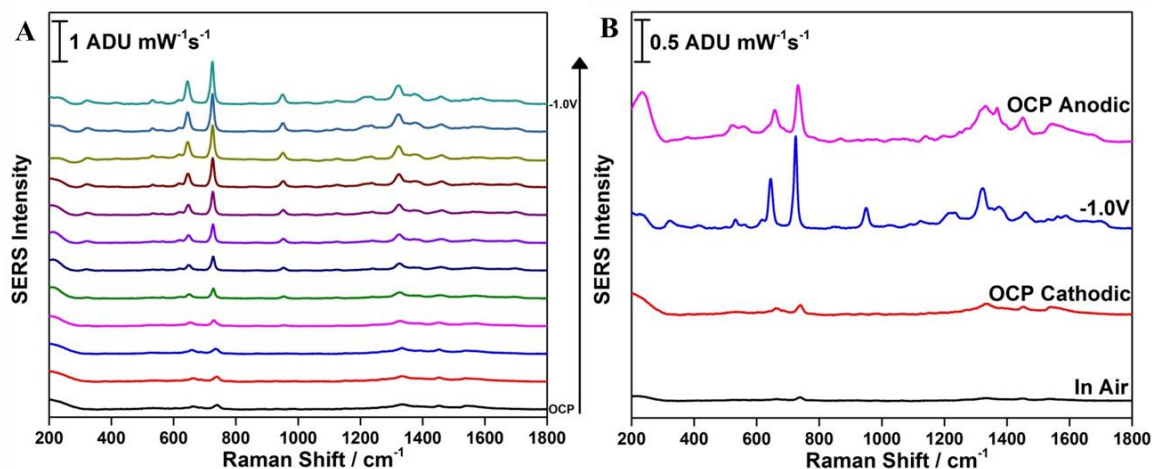
Figure 2.2.10: (A) Cathodic progression of the SERS spectra and (B) EC-SERS comparison for a mixture of all seven breakdown products on silver using an excitation wavelength of 780 nm with a laser power of 80 mW for an acquisition time of 30 seconds.

2.3 EC-SERS of Bacteria

2.3.1 *Escherichia coli* K-12

The *Escherichia coli (E. coli)* K-12 strain of bacteria was used to optimize EC-SERS measurement conditions for bacterial screening, as *E. coli* is a prime target pathogenic bacterium which is currently one of the two most commonly detected strains of bacteria, although a non-pathogenic strain (K-12) was used in this thesis work. The first studies that were attempted used the drop coating method to place bacteria suspended in water (prepared as outlined in the methods section) on the surface of the WE of the SPE, as is typically done for probe molecules, and as was done for the characterization of the nucleotide breakdown products. The spectra of bacteria collected using this drop coating method yielded no useful peaks, so it was expected that the bacteria were floating away from the surface of the electrode when immersed in the pH 7.4 phosphate buffer

used as the supporting electrolyte. This was one of the main hurdles to overcome while developing an EC-SERS method for bacterial screening, achieving good adhesion between the substrate and the bacteria such that the bacteria is not displaced by the addition of a supporting electrolyte.

After moving on from the unsuccessful drop coating method, a method similar to that described by Mosier-Boss *et al.* was attempted, where a mixture of aqueous bacterial suspension and citrate-reduced AgNPs were mixed together prior to EC-SERS measurement.[30] In this experiment, an equal mixture of AgNP colloid with aqueous bacterial suspension was allowed to equilibrate for one hour, centrifuged to concentrate, and three layers of 5.0 µL of the concentrated solution was applied to the WE of the SPE. The results of this study are shown in Figure 2.3.1.1, where A shows the cathodic progression of the SERS signal of bacteria, showing no response to applied voltage. Figure 2.3.1.1 B shows the EC-SERS comparison of the signal, showing no improvement with EC-SERS over normal SERS. The bacteria/AgNP mixture on the WE also did not dry properly, and had a sludge-like appearance, which was unstable once phosphate buffer was added. This method was also deemed inappropriate for bacterial screening using EC-SERS, as the signal did not benefit from the application of a negative WE potential likely due to the weak adsorption of the bacteria at the electrode surface.
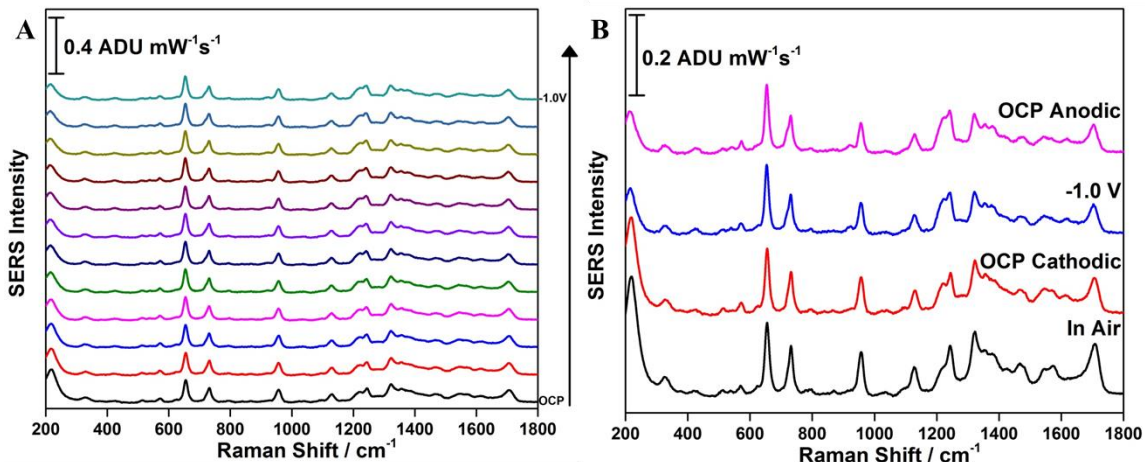
Figure 2.3.1.1: (A) Cathodic progression of the SERS signal and (B) EC-SERS comparison for a mixture of *E. coli* K-12 bacteria and AgNPs using the 780 nm excitation laser line with a laser power of 80 mW and an acquisition time of 30 seconds.

As it was clear that achieving good adhesion between the bacteria and the WE was required, several surface functionalization strategies were attempted, where the AgNPs on the WE were modified with pyridine and cysteamine (separately). With the pyridine functionalization, it was expected that the nitrogen would bind to the silver nanoparticles, potentially allowing for an interaction between the π electrons of the pyridine ring and the bacterial cells. With the cysteamine functionalization, it was expected that the thiol group would bind to the silver nanoparticles, potentially allowing for an interaction between the amine group and the bacterial cells. The hope was that either of these cases would hold the bacteria cells tightly to the surface of the WE, such that they would not be displaced upon the addition of phosphate buffer electrolyte for EC-SERS measurements. This, however, was not the case, and both methods yielded weak signals. Figure 2.3.1.2 A shows the EC-SERS comparison for one of the trials of pyridine surface

functionalization. B shows the EC-SERS comparison for one of the trials of cysteamine surface functionalization.
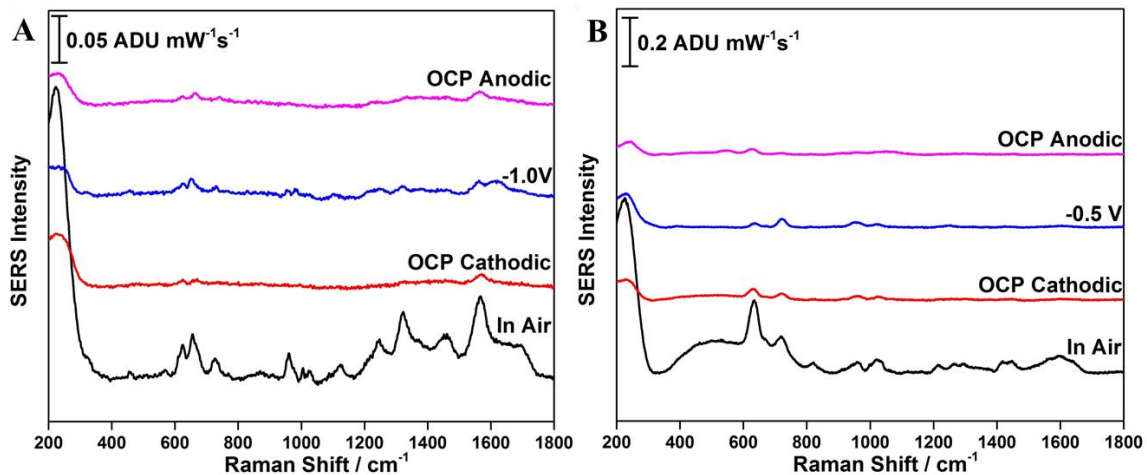
Figure 2.3.1.2: (A) EC-SERS comparison for pyridine functionalized silver substrate and (B) EC-SERS comparison for cysteamine functionalized silver substrate for *E. coli* K-12 collected using a 780 nm excitation laser line with a laser power of 80 mW and an acquisition time of 30 seconds.

For EC-SERS of bacteria, while many preparation methods were attempted, the most promising method was found to be incubating the KCl treated electrode in an aqueous bacterial suspension overnight and allowing the electrode to air dry for several minutes prior to beginning EC-SERS measurements. Figure 2.3.1.3 A shows the cathodic progression of the SERS spectra of *E. coli* K-12 when this method was used. This demonstrates that the result of an applied potential was a significantly improved SERS signal. Figure 2.3.1.3 B shows the EC-SERS comparison for *E. coli* K-12 on silver using the 780 nm laser, where it is demonstrated that applied voltage can significantly enhance the SERS spectrum of bacteria. Figure 2.3.1.4 shows the optimized negative EC-SERS

39

spectra for bacteria using this method for four trials to show the reproducibility of the method.

Figure 2.3.1.3: (A) Cathodic progression of the SERS spectra and (B) EC-SERS comparison of *E. coli* K-12 on silver deposited using the incubation method in water using a 780 nm laser line with a laser power of 80 mW and an acquisition time of 30 seconds.
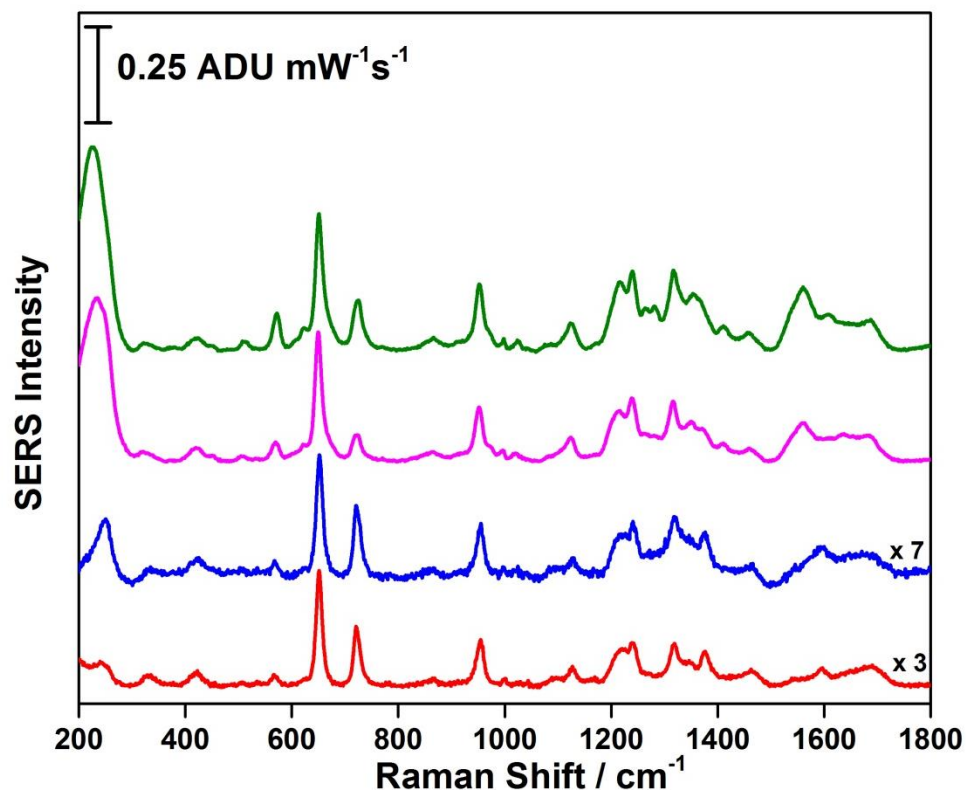
Figure 2.3.1.4: Optimized negative EC-SERS spectra for *E. coli* K-12 bacteria using the incubation method (in water) for five separate trials on silver substrates using a 780 nm laser line with a laser power of 80 mW and an acquisition time of 30 seconds.

While the results obtained for the incubation method were satisfactory, the incubation studies were repeated with the only difference being that phosphate buffer was used in place of water for the incubation. Due to time constraints, only three studies were done as opposed to the four studies done with the water incubation. This method adjustment provided an improvement in terms of SERS spectral quality and reproducibility. Figure 2.3.1.5 shows an example of an experiment using phosphate buffer as the incubation media with A showing the cathodic progression of the SERS signal and B showing the EC-SERS comparison. Figure 2.3.1.6 shows the optimized negative EC-SERS spectra for bacteria using this method for three trials to show the very good

reproducibility of the relative spectral peak intensities. For both methods, EC-SERS was able to amplify the normal SERS signal by factors upwards of 10. It should be noted that the reproducibility of the SERS peak intensity is very poor for both the water and phosphate buffer incubation methods, suggesting that both methods are unsuitable for quantitative detection in their current states.

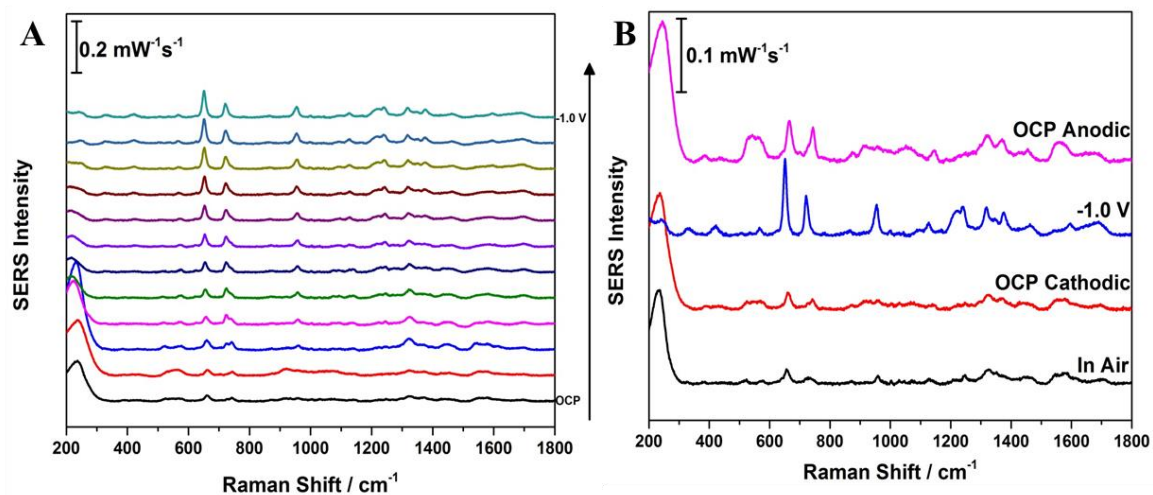**Figure 2.3.1.5:** (A) Cathodic progression of the SERS spectra and (B) EC-SERS comparison of *E. coli* K-12 on silver deposited using the immersion method in phosphate buffer using a 780 nm laser line with a laser power of 80 mW and an acquisition time of 30 seconds.
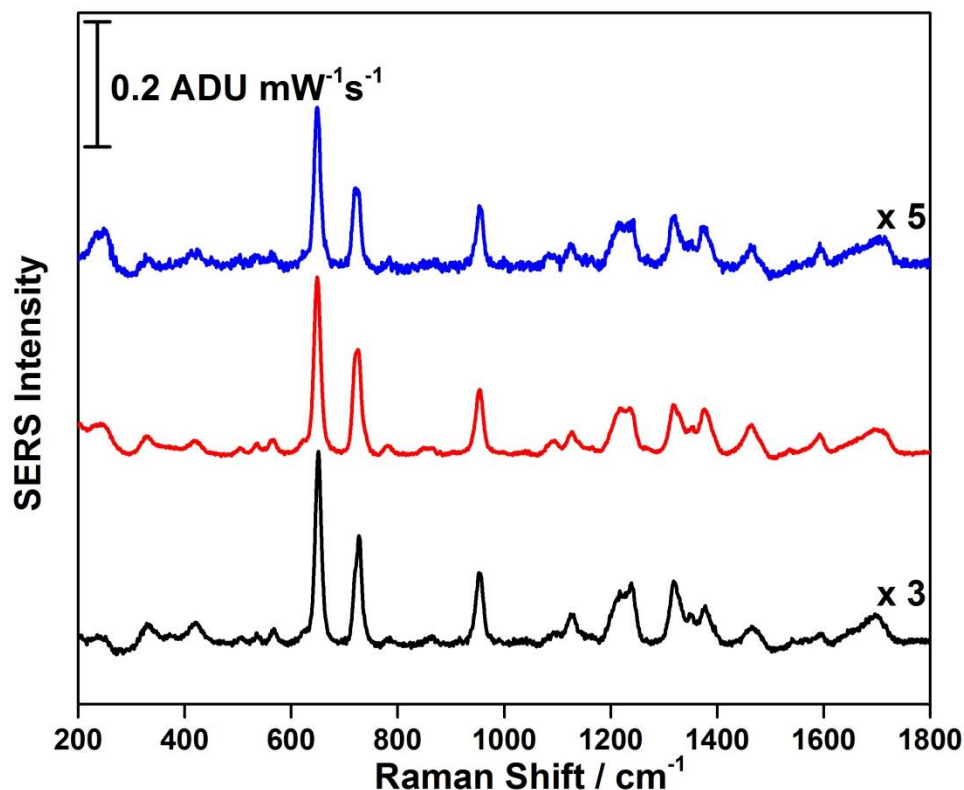
Figure 2.3.1.6: Optimized negative EC-SERS spectra for *E. coli* K-12 bacteria using the immersion method (in phosphate) for three separate trials on silver substrates using a 780 nm laser line with a laser power of 80 mW and an acquisition time of 30 seconds.

The great improvement of EC-SERS over normal SERS for the detection of bacteria can likely be attributed to a number of factors. The chloride peak at 240 cm^{-1} disappears as the potential is stepped more negative, as it is desorbed from the surface of the electrode, which then likely allows the bacteria to better access the surface of the WE.[9] The metal surface becomes less positively charged as the potential is stepped in the negative (cathodic) direction (potential of zero charge for Ag = -0.95 V vs Ag/AgCl), causing the negatively charged chloride molecules to desorb from the surface at approximately -0.5 V, where the Ag-Cl peak disappears.[9] EC-SERS is also known to simulate more biologically relevant electric field conditions, which may encourage the bacteria to adhere to the surface of the electrode more than it would with regular SERS.

43

An SEM image of the surface of the WE of the SPE after EC-SERS analysis (Figure 2.3.1.7) shows the bacteria on the AgNP coated surface. The *E. coli* K-12 bacteria are rod-like, and appear as dark shadows in the SEM image. Based on the SEM images of the WE after EC-SERS measurements were obtained, it is clear that there were not many bacterial cells on the surface, so EC-SERS is able to detect quite a small number of cells. Assuming a 25 μm laser spot diameter at focus, on average there are approximately 8 *E. coli* K-12 bacterial cells in the area for which a SERS spectrum is collected.

| SEM HV: 5.0 kV | WD: 9.55 mm | | MIRA3 TESCAN |
| View field: 39.9 μm | Det: SE | 10 μm | |
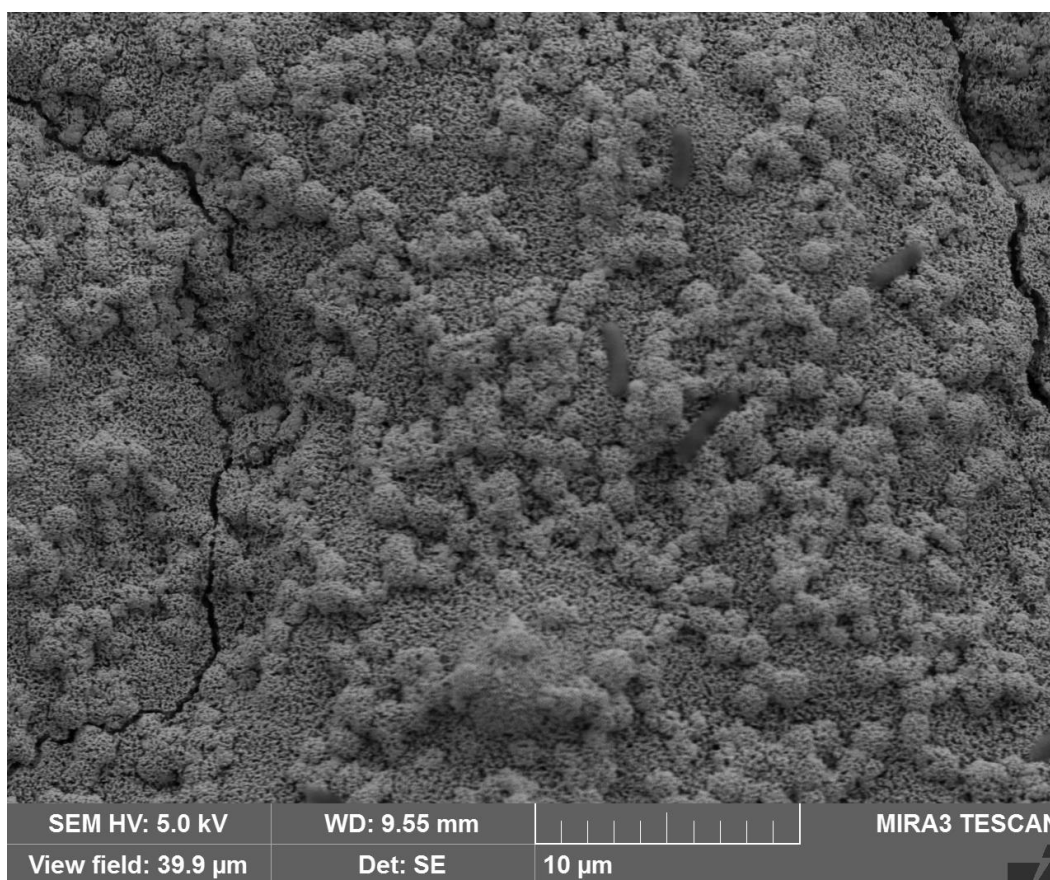
Figure 2.3.1.7: SEM image showing the surface of the WE with four *E. coli* K-12 bacterial cells taken at 5.0 kV.

2.3.2 *Bacillus megaterium*

After optimizing the experimental conditions for the immersion method of bacterial deposition onto the WE with *E. coli*, it was important to establish if this method

could be applied to other strains of bacteria to achieve EC-SERS profiling. To test this, *B. megaterium* was used, which is a Gram-positive strain of bacteria.[53] The EC-SERS data could also be used as a means of comparison with the EC-SERS data for *E. coli* to determine if EC-SERS is able to differentiate between Gram-positive and Gram-negative strains of bacteria. Figure 2.3.2.1 A shows the cathodic progression of the SERS spectrum and B shows the EC-SERS comparison for *B. megaterium* which was deposited onto a silver electrode using the immersion method. The cathodic progression of the SERS spectrum shows that the signal for *B. megaterium* benefits from the application of a negative potential, as was observed for *E. coli*. The optimized negative EC-SERS spectrum is -1.0 V, with the strongest signal being present at this potential. The EC-SERS comparison shows the improvement of the signal from the normal SERS spectrum (the in air spectrum) to the spectrum at -1.0 V. These results showed promise for EC-SERS for bacterial screening, as two strains of bacteria with different cell walls behaved similarly to the application of voltage to the surface of the EC-SERS substrate. This indicates that this method can be used to screen for multiple strains of bacteria without significant alteration of the method.
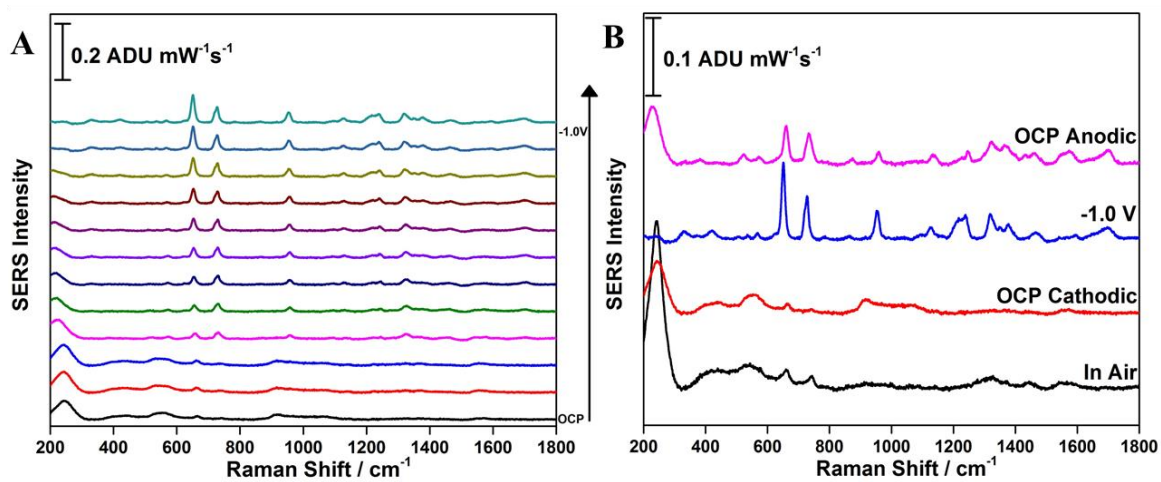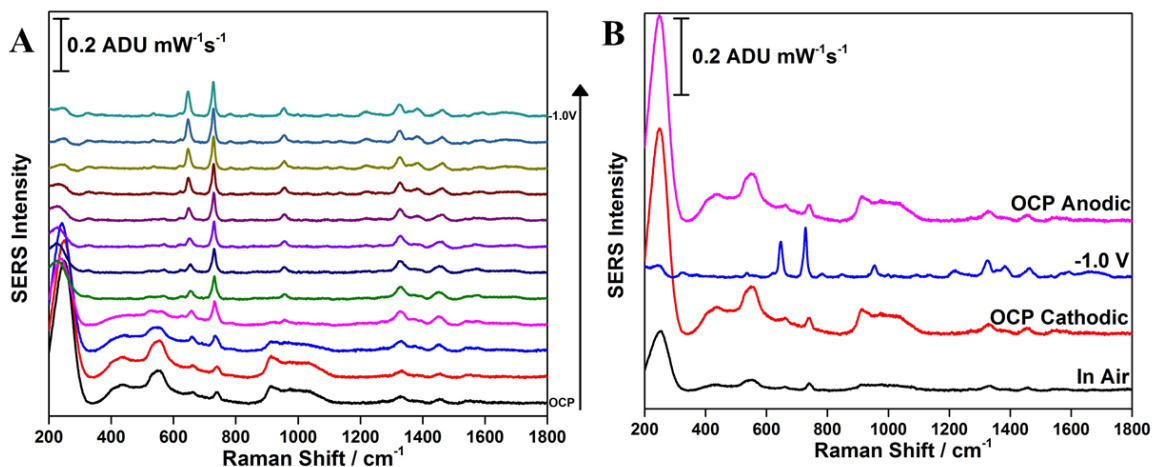
Figure 2.3.2.1: (A) Cathodic progression of the SERS spectra and (B) EC-SERS comparison of *B. megaterium* on silver deposited using the immersion method in phosphate buffer using a 780 nm laser line with a laser power of 80 mW and an acquisition time of 30 seconds.

It was important to investigate the reproducibility of the EC-SERS signal produced using this method with *B. megaterium*. Figure 2.3.2.2 shows a comparison of the optimized negative spectra (at -1.0 V) for three separate experiments done using the immersion method of *B. megaterium* for EC-SERS screening. As was previously demonstrated with *E. coli*, the SERS spectrum obtained for *B. megaterium* was found to be reproducible. An SEM image of the surface of the WE of the SPE after EC-SERS analysis (Figure 2.3.2.3) shows the bacteria on the AgNP coated surface. The *B. megaterium* bacteria are rod-like, and appear as dark shadows in the SEM image. Based on the SEM images of the WE after EC-SERS measurements were obtained, it is again clear that there were not many bacterial cells on the surface, so EC-SERS is able to detect quite a small number of cells as observed for *E. coli*. Assuming a 25 μm laser spot diameter at focus, on average there are approximately six *B. megaterium* bacterial cells in the area for which a SERS spectrum is collected, which is close to the average amount of

E. coli K-12 cells that were within the laser spot. As was the case with *E. coli*, the spectral

intensities for the SERS signals of *B. megaterium* were not reproducible.
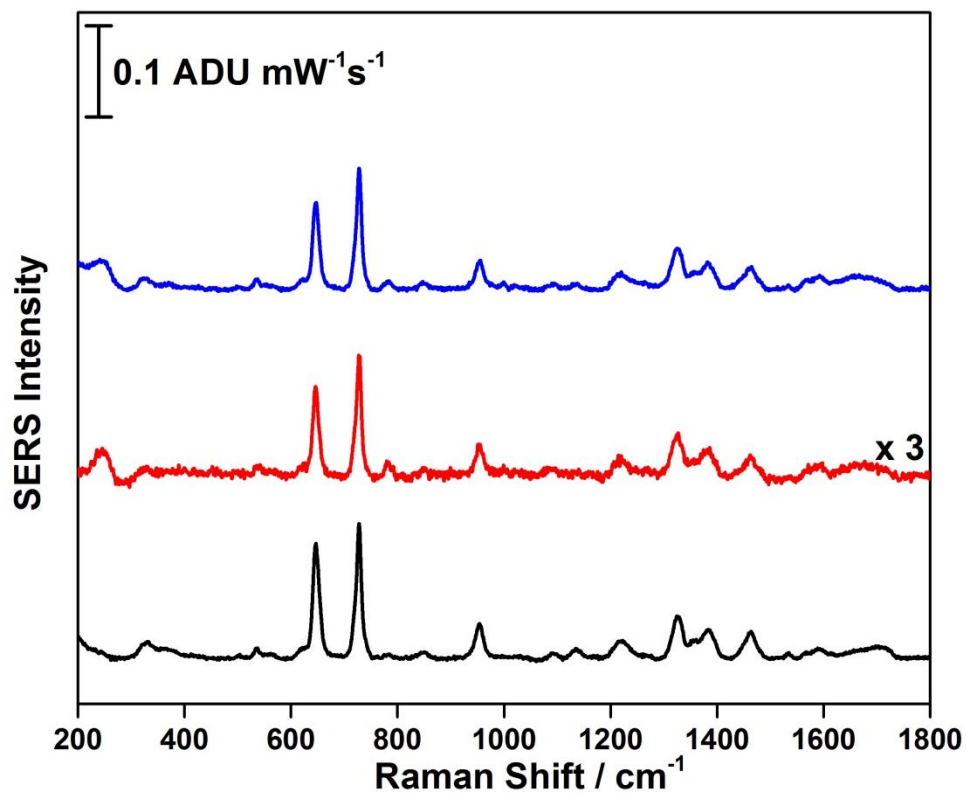
Figure 2.3.2.2: Optimized negative EC-SERS spectra for *B. megaterium* bacteria using the immersion method (in phosphate buffer) for three separate trials on silver substrates using a 780 nm laser line with a laser power of 80 mW and an acquisition time of 30 seconds.
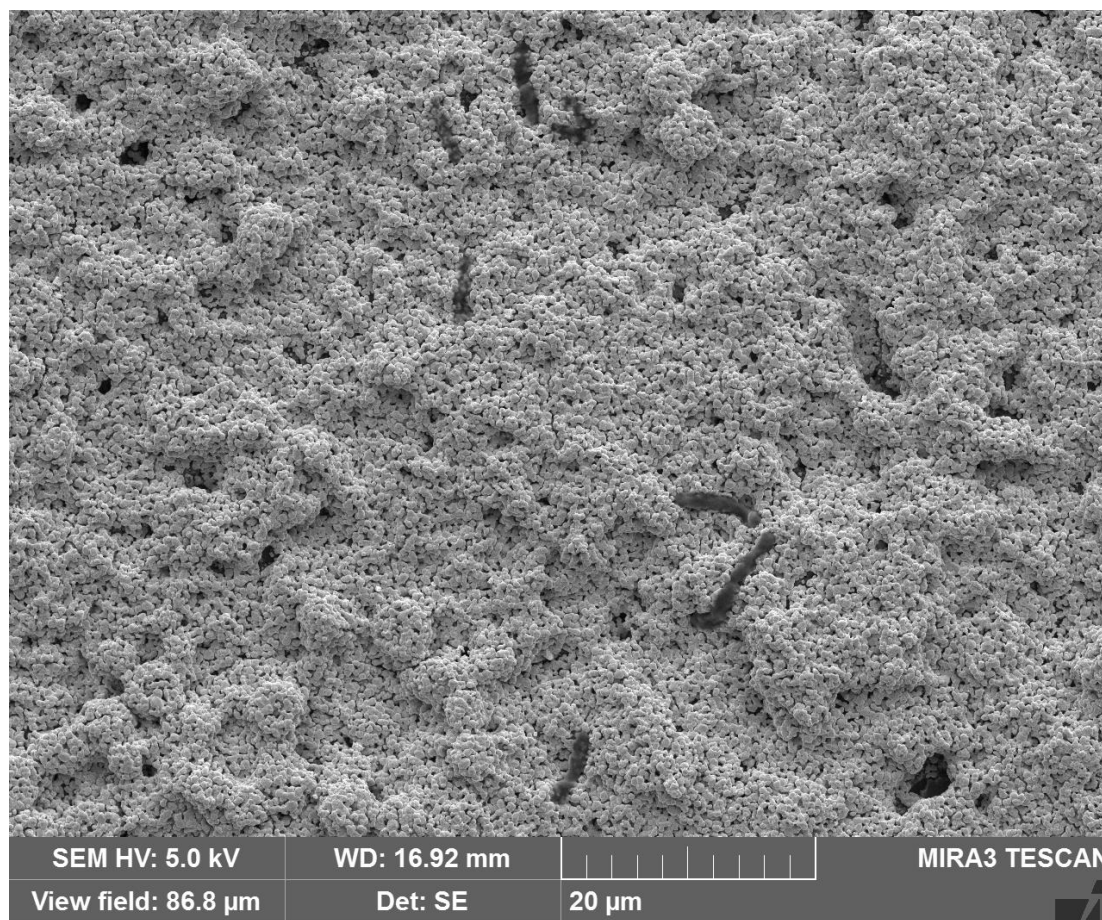
Figure 2.3.2.3: SEM image showing the surface of the WE with six *B. megaterium* bacterial cells.

2.4 Comparison of Bacterial Spectra with Breakdown Products

Figure 2.4.1 shows an overlay of the average spectrum of *E. coli* collected using the immersion method in phosphate buffer with those of the nucleotide breakdown products with the spectral intensities scaled for ease of comparison. The similarities between the *E. coli* spectrum and those of the breakdown products are visually evident. Visual analysis, however, is not a reliable means of spectral comparison, as it is only qualitative and prone to human error. Therefore, in order to compare the EC-SERS spectra obtained for bacteria to the spectra of the seven nucleotide breakdown products, a

library database was constructed using Omnic® Specta containing the optimized negative EC-SERS spectra of the seven products of nucleotide degradation. By using software to compare the spectra, a quantitative result can be obtained that is not prone to operator error. The bacterial EC-SERS spectra could be run through this database to determine the percent match with each of the spectra in the database (the spectra of the nucleotide breakdown products). The percent match was generated based on the similarity of the spectral peaks. Table 2.4.1 shows the results of running three optimized negative EC-SERS spectra (-1.0 V spectra) of *E. coli* through the database. It was found that the major contributors to the spectrum of *E. coli* were xanthine and guanine, with 80% and 74% matches, respectively. The results of Table 2.4.1 are visually represented as pie charts in Figure 2.4.2.

Figure 2.4.1: Overlay of average spectrum of *E. coli* collected using the immersion method in phosphate buffer with those of the nucleotide breakdown products on silver substrates using the 780 nm laser line at a power of 80 mW with an acquisition time of 30 seconds.

Table 2.4.1: Contributions of EC-SERS spectra of nucleotide breakdown products to the EC-SERS spectra of *E. coli* collected using the immersion method in phosphate buffer.

Nucleotide Breakdown Product	% match with *E. coli* spectrum 1	% match with *E. coli* spectrum 2	% match with *E. coli* spectrum 3	Average (%)
Adenine	40	38	28	35 ± 6
Guanine	70	81	72	74 ± 6
Xanthine	83	82	75	80 ± 4
Hypoxanthine	40	47	36	41 ± 6
AMP	3	5	5	6 ± 1
Uric Acid	4	4	5	4 ± 1
Guanosine	39	57	50	49 ± 9

Figure 2.4.2: Pie chart depicting the relative contributions of each nucleotide breakdown product to the SERS spectrum for *E. coli*.

Figure 2.4.2 shows an overlay of the average spectrum of *B. megaterium* collected using the immersion method in phosphate buffer with those of the nucleotide breakdown products. The results in Table 2.4.2 show that the major contributor to the EC-SERS

spectrum of *B. megaterium* was adenine with a 74% match. Xanthine, hypoxanthine, and guanine all contributed approximately equally to the *B. megaterium* spectrum, with percent match values of ~50%. The results of Table 2.4.2 are visually represented as a pie chart in Figure 2.4.4.
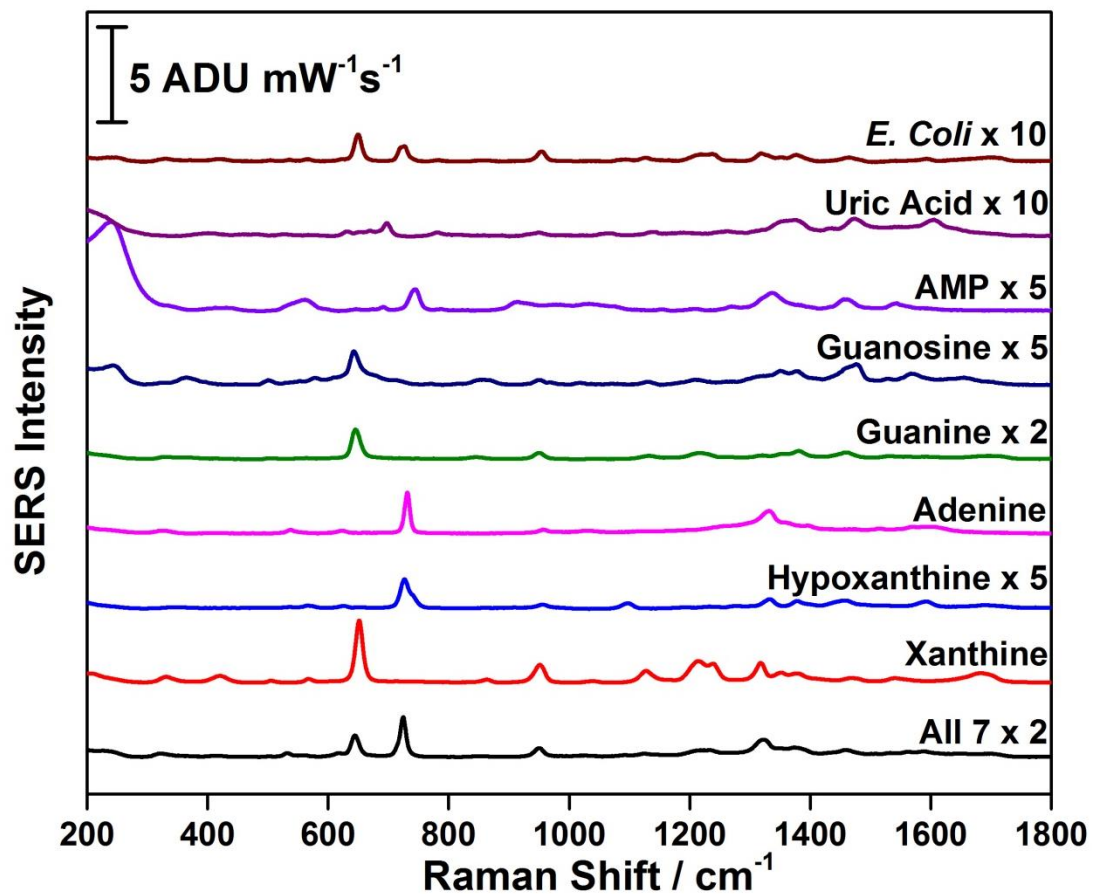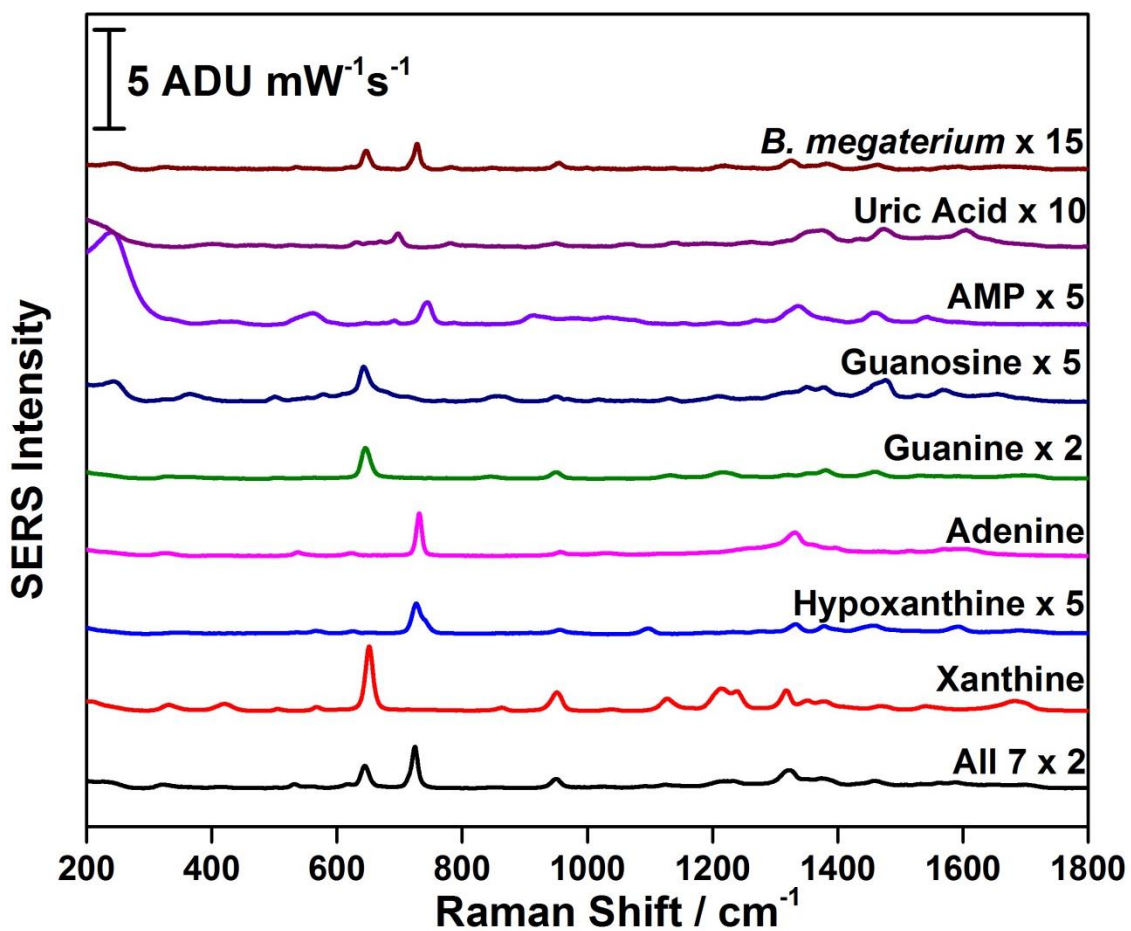

Figure 2.4.3: Overlay of average spectrum of *B. megaterium* collected using the immersion method in phosphate buffer with those of the nucleotide breakdown products on silver substrates using the 780 nm laser line at a power of 80 mW with an acquisition time of 30 seconds.

Table 2.4.2: Contributions of EC-SERS spectra of nucleotide breakdown products to the EC-SERS spectra of *B. megaterium* collected using the immersion method in phosphate buffer.

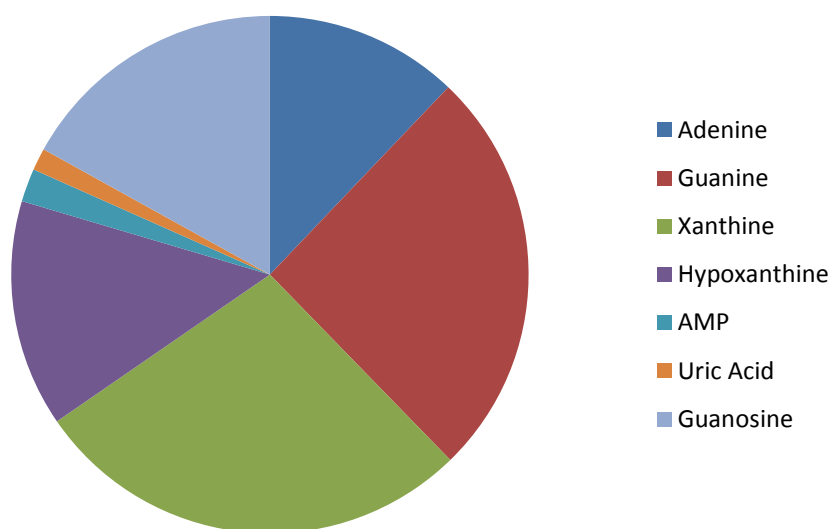| Nucleotide Breakdown Product	% match with *B. megaterium* spectrum 1	% match with *B. megaterium* spectrum 2	% match with *B. megaterium* spectrum 3	Average (%) (excluding results from spectrum 3)
Adenine	70	78	74	74 ± 4
Guanine	49	54	62	55 ± 7
Xanthine	44	49	55	49 ± 6
Hypoxanthine	52	58	54	55 ± 3
AMP	9	11	6	9 ± 3
Uric Acid	4	5	4	4 ± 1
Guanosine	41	47	47	45 ± 4
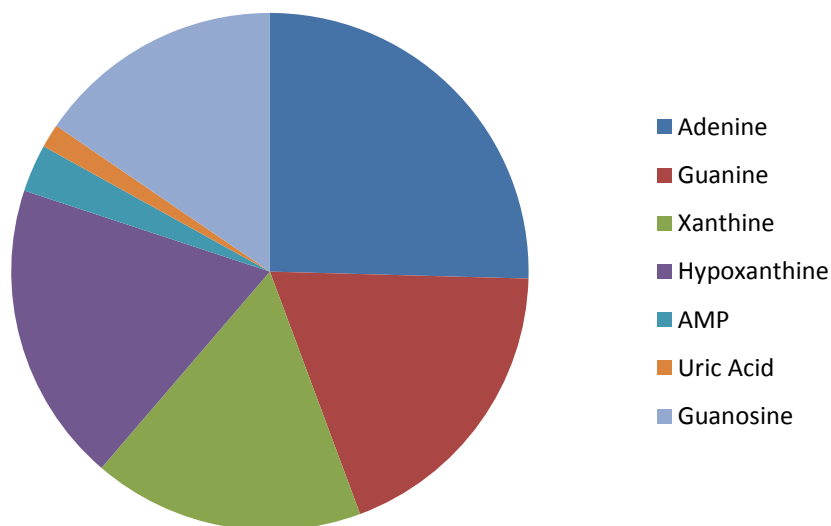
Figure 2.4.4: Pie chart depicting the relative contributions of each nucleotide breakdown product to the SERS spectrum for *B. megaterium.*

The above results show that by using a database of the EC-SERS spectra of the seven nucleotide breakdown products that contribute to the spectrum of bacteria, the strains *E. coli* and *B. megaterium* can be differentiated. The spectra of *E. coli* can be identified by having matches of approximately 80% with xanthine and approximately 75% with guanine. The spectra of *B. megaterium*, however, matches approximately 75% with adenine, while the spectrum of E. coli only matched about 35% with adenine. Another notable difference is that xanthine and guanine match only about 50% with the spectrum of *B. megaterium*. The spectra of both bacteria had low spectral matches with uric acid and AMP, indicating that they either contribute very little to the EC-SERS spectrum of bacteria, or their contributions are too weak in terms of spectral intensities to be visible in the spectrum that is dominated by the stronger spectral peaks of the other breakdown products.

Chapter 3: Conclusion

This thesis work explored EC-SERS as a method for bacterial screening for the first time. After trying several methods of preparing the substrate with bacteria for EC-SERS, it was determined that it was necessary to achieve good adhesion between the bacterial cells and the substrate. A method for the deposition of bacterial cells onto the surface of the EC-SERS substrate was successfully developed, proving to be applicable to the Gram-negative bacterial strain *E. coli* and the Gram-positive strain *B. megaterium*. The method that was able to allow for adequate adhesion between the bacteria and the substrate involved immersion of the substrate in a suspension of bacteria in phosphate buffer and incubating the immersed substrate at room temperature, then allowing the substrate to air dry prior to EC-SERS measurements. The results of the EC-SERS studies of bacteria showed that the SERS spectrum could be greatly improved by means of an applied voltage. The SERS spectra obtained for both strains of bacteria were shown to be attributed to seven products of nucleotide breakdown; adenine, guanine, xanthine, hypoxanthine, AMP, uric acid, and guanosine. All seven of this breakdown products, as well as an equal mixture of all seven products were fully characterized using EC-SERS, providing a useful database for the comparison of the EC-SERS spectra of these molecules with the spectra produced by bacteria. It was shown that it was possible to differentiate between the EC-SERS spectra of *E. coli* and *B. megaterium* bacteria by comparing the spectra to a database containing the spectra of the seven nucleotide breakdown products and analyzing the major contributors to the bacterial signal. The EC-SERS spectra of *E. coli* were found to match most with the EC-SERS spectra for xanthine and guanine, where the EC-SERS spectra of *B. megaterium* were found to match most

with the EC-SERS spectrum of adenine. This thesis work provides a new method for bacterial detection, demonstrating how to improve upon the already promising method of SERS for bacterial screening by using EC-SERS.

Chapter 4: Future Work

For future work, principle component analysis coupled with hierarchical cluster analysis should be used to differentiate between strains of bacteria, as multivariate statistical analysis has proven to be useful for bacterial strain differentiation using SERS. Additionally, surface modifications to the nanoparticles on the surface of the working electrode on the screen printed electrode should be explored to achieve better adhesion between the bacteria and the surface of the electrode and to achieve a higher surface concentration of bacteria for EC-SERS analysis, such as functionalizing the nanoparticles with an aptamer. A key future goal for this project is to be able to apply this bacterial detection platform to real world samples, so experiments should be carried out in biologically, industrially, and environmentally relevant samples such as synthetic urine, food samples, and water samples. A time study should also be carried out to observe the effects of reducing the amount of time for which the electrode is incubated in a suspension of bacteria in phosphate buffer, with the goal of reducing that time as much as possible for PON bacterial screening. Additionally, in order for this method to be quantitative in nature, the signal intensity reproducibility will have to be improved before the signal intensity can be related to bacterial concentration. Other bacterial strains, such as multiple *Escherichia* and *Bacillus* strains, should also be investigated in order to further evaluate EC-SERS as a method for bacterial strain identification.

Chapter 5: Experimental

5.1 Reagents and Materials

Potassium phosphate dibasic (>98%) and agar powder (lab grade) were purchased from Anachemia Canada (Montréal, QC, CA) and potassium phosphate (>99%) was purchased from ACP Chemicals (Montréal, QC, CA). Silver nitrate (99.9995%) was purchased from Alfa Aesar (Ward Hill, MA, USA). Sodium chloride, pyridine, and tryptone (bacteriological) were purchased from VWR International (Solon, OH, USA). Microbiology Fermtech® yeast extract was purchased from EMD Millipore Corporation (Billerica, MA, USA). Ethanol (95%), potassium chloride ($\geq$99%), hypoxanthine (>99%), guanosine ($\geq$98%), guanine (98%), xanthine ($\geq$99%), uric acid (>99%), adenosine 5' mono-phosphate disodium salt (AMP) (>99%), cysteamine (>98%), lipopolysaccharides from E. coli (phenol extraction purification), adenine ($\geq$99%) were purchased from Sigma Aldrich (St, Louis, MO, USA). A culture of *Escherichia coli* (*E. coli*) K-12 was obtained Bio Rad Laboratories (Hercules, CA, USA) and a culture of *Bacillus megaterium* (*B. megaterium*) was obtained from Boreal Scientific (St. Catherines, ON, CA). All chemicals were used as received without further purification. All solutions were prepared using Millipore water (solution resistivity $\geq$18.2 MΩ cm). Glassware was cleaned in neat sulfuric acid and thoroughly rinsed with Millipore water prior to use. Screen printed electrodes used to fashion the SERS substrates and the WaveNow Potentiostat/Galvanostat System used for EC-SERS were purchased from Pine Research Instrumentation (Durham, NC, USA).

5.2 Microscopic Studies

The electrodes were imaged using a TESCAN MIRA 3 LMU Variable Pressure Schottky Field Emission Scanning Electron Microscope (FE-SEM), with a maximum resolution of 1.2 nm at 30 kV. Electrodes containing bacteria were dried using 95% Ethanol prior to imaging. SEM image processing was done with the assistance of ImageJ software (NIH, Maryland, USA).

5.3 Spectroscopic and Spectroelectrochemical Studies

EC-SERS measurements were collected using a DXR Smart Raman spectrometer equipped with 780 nm and 532 nm lasers (Thermo Fisher Scientific, Mississauga, ON, Canada). The spectrometer resolution is 3 cm^{-1} and it is equipped with an air-cooled CCD detector. The DXR Smart Raman spectrometer is coupled to a Pine Research Instrumentation portable USB Wavenow potentiostat/galvanostat (Durham, NC, USA) to perform EC-SERS measurements using phosphate buffer as an electrolyte. For EC-SERS, the applied potential ranges from 0.4 V to -1.0 V vs. Ag/AgCl in increments of 0.1 V, all potentials are vs. Ag/AgCl. All spectra were corrected for laser power and acquisition time for ease of comparison, and were baseline corrected using the NuSpec software. Data was analyzed using Origin 9.0 software (OriginLab Corporation, Northampton, MA, USA).

5.4 Silver Nanoparticle (AgNP) Synthesis

1.0 mL of silver nitrate solution (0.1 M), 3.4 mL of aqueous sodium citrate (5%), and 0.6 mL of citric acid (0.17 M) were added into a 250 mL three-neck flat-bottom flask with 95.0 mL of water. 0.2 mL of freshly prepared sodium borohydride solution (0.1 mM)

was then added into the above mixture at room temperature under magnetic stirring. The mixture was allowed to stand at room temperature for 1 min and then brought to boil under reflux within 20 min under magnetic stirring. After boiling for 1 h, the dark yellow solution was allowed to cool to room temperature. To concentrate the AgNPs, aliquots of the colloidal suspension were added to Eppendorf tubes, which were then centrifuged at 8,000 rpm for 20 minutes (Labnet PRISM microcentrifuge, Edison, NJ, USA). The supernatant was then removed and discarded, and the remaining paste put into one tube and centrifuged again. The final paste was adjusted to a concentration of 0.4 M with water.

5.5 Gold Nanoparticle (AuNP) Synthesis

1.0 mL of $HAuCl_4$ solution (25 mM) was added to a 250 mL three-neck flat-bottom flask with 98 mL of water. After the solution was brought to a boil under reflux and mechanical stirring, 1 mL of sodium citrate (5%) solution was added. After boiling for 20 minutes, the wine red solution was allowed to cool to room temperature. The AuNPs were concentrated to a 0.4 M paste by the same method as for the AgNPs that is described above.

5.6 Preparation of EC-SERS Substrates

Screen printed electrodes were modified with nanoparticles for use in EC-SERS sensing. Three layers of the AgNP paste were drop coated onto the working electrode surface of a carbon screen printed electrode in 5 µL aliquots, drying fully between layers. Using three layers of the AgNP paste was found to be the optimal amount to ensure uniform surface coverage. The electrodes were then immersed in 0.5 M KCl for 30

minutes to remove citrate, rinsed with ultrapure water and dried prior to application of the probe. 5.0 µL of the probe molecule solution was then deposited onto the modified electrode surface and allowed to dry prior to spectroscopic studies.

5.7 Preparation of Bacteria Samples

A single colony of bacteria was taken from a nutrient agar plate stored at room temperature and transferred into a disposable plastic tube containing 10 mL of nutrient broth. The tube was then loosely capped and incubated at 37°C, rotating at approximately 120 rpm for 16 – 20 hours. The resulting cloudy bacterial solution was then centrifuged using the same equipment as described above for 10 minutes at 4000 rpm once to remove the supernatant, and three additional times with water to remove the remaining growth medium. For immersions in phosphate buffer, the last of the three rinse cycles were completed using phosphate buffer in place of water. The result was a concentrated pellet of bacteria cells.

5.8 Bacteria Immersion Method

A concentrated bacterial pellet obtained using the procedure described above was re-suspended in 5.0 mL of water or phosphate buffer in a disposable glass vial. A prepared screen printed electrode was then immersed in the bacterial suspension and incubated at room temperature overnight. After 16 hours, the electrode was removed and allowed to dry prior to spectroscopic studies.

Chapter 6: References

1. Ahmed, A.; Rushworth, J. V.; Hirst, N.A.; Millner, P.A. Biosensors for Whole-Cell Bacterial Detection. *Clin. Microbiol. Rev.* **2014**, *27*, 631-646.

2. Lazcka, O.; Del Campo, F.J.; Muñoz, F.X. Pathogen detection: A perspective of traditional methods and biosensors. *Biosens. Bioelectron.* **2007**, *22*, 1205-1217.

3. Bumbrah, G. S.; Sharma, R. M. Raman spectroscopy − Basic principle, instrumentation and selected applications for the characterization of drugs and abuse. *Egypt. J. Forensic Sci.* **2016**, *6*, 209-215.

4. Schlücker, S. Surface-Enhanced Raman Spectroscopy: Concepts and Chemical Applications. *Angew. Chem. Int. Ed.* **2014**, *53*, 4756-4795.

5. Olson, A. P.; Spies, K. B.; Browning, A. C.; Soneral, P. A. G.; Lindquist, N. C. Chemically imaging bacteria with super-resolution SERS on ultra-thin silver substrates. *Sci. Rep.* **2017**, *7*:9135.

6. Zhang, Q.; Wang, X. -D.; Tian, T.; Chu, L. -Q. Incorporation of multilayered silver nanoparticles into polymer brushes as 3-dimensional SERS substrates and their application for bacteria detection. *Appl. Surf. Sci.* **2017**, *407*, 185-191.

7. Premasiri, W. R.; Lee. J. C.; Sauer-Budge, A.; Théberge, R.; Costello, C. E.; Ziegler, L. D. The biochemical origins of the surface-enhanced Raman spectra of bacteria: a metabolomics profiling by SERS. *Anal. Bioanal. Chem.* **2016**, *408*, 4631-4647.

8. Patel, I. S.; Premasiri, W. R.; Moir, D. T.; Ziegler, L. D. Barcoding bacterial cells: a SERS-based methodology for pathogen identification. *J. Raman Spectrosc.* **2008**, *39*, 1660-1672.

9. Karaballi, R. A.; Nel, A.; Krishnan, S.; Blackburn, J.; Brosseau, C. L. Development of an electrochemical surface-enhanced Raman spectroscopy (EC-SERS) aptasensor for direct detection of DNA hybridization. *Phys. Chem. Chem. Phys.* **2015**, *17*, 21356-21363.

10. Greene, B. H. C.; Alhatab, D. S.; Pye, C. C.; Brosseau, C. L. Electrochemical-Surface Enhanced Raman Spectroscopic (EC-SERS) Study of 6-Thiouric Acid: A Metabolite of the Chemotherapy Drug Azathioprine. *J. Phys. Chem. C.* **2017**, *121*, 8084-8090.

11. Ivnitski, D.; Abdel-Hamid, I.; Atanasov, P.; Wilkins, E. Biosensors for detection of pathogenic bacteria. *Biosens. Bioelectron*. **1999**, *14*, 599-326.

12. Teng, J.; Yuan, F.; Ye, Y.; Zheng, L.; Yao, L.; Xue, F.; Chen, W.; Li, B. Aptamer-Based Technologies in Foodborne Pathogen Detection. *Front. Microbiol*. **2016**, *7*:1426. Hamadi, F.; Latrache, H.; Zahir, H.; Elghmari, A.; Timinouni, M.; Ellouali, M. The relationship between Escherichia coli surface functional groups' composition and their physicochemical properties. *Braz. J. Microbiol.* **2008**, *39*, 10-15.

13. Cho, I. –H.; Bhandari, P.; Patel, P.; Irudayaraj, J. Membrande filter-assisted surface-enhanced Raman spectroscopy for the rapid detection of E. coli 0157:H7 in ground beef. *Biosens. Bioelectron*. **2015**, *64*. 171-176.

14. Paniel, N.; Baudart, J.; Hayat, A.; Barthelmebs, L. Aptasensor and genosensor methods for detection of microbes in real world samples. *Methods*. **2013**, *64*, 229-240.

15. Song, S.; Wang, L.; Li, J.; Zhao, J.; Fan, C. Aptamer-based biosensors. *Trends Anal. Chem.* **2008**, *27*, 108-117.

16. Alocilja, E. C.; Radke, S. M. Market analysis of biosensors for food safety. *Biosens. Bioelectron.* **2003**, *18*, 841-846.

17. Taylor, A. J.; Lappi, V.; Wolfgang, W.J.; Lapierre, P.; Palumbo, M.J.; Medus, C.; Boxrud, D. Characterization of Foodborne Outbreaks of *Salmonella enterica* Serovar Enteritidis with Whole-Genome Sequencing Single Nucleotide Polymorphism-Based Analysis for Surveillance and Outbreak Detection. *J. Clin. Microbiol.* **2015**, *53*, 3334-3340.

18. Välimaa, A. -L.; Tilsala-Timisjärvi, A.; Virtanen, E. Rapid detection and identification methods for *Listeria monocytogenes* in the food chain − A review. *Food Control.* **2015**, *55*, 103-114.

19. Hinks, J.; Han, E. J. Y.; Wang, V. B.; Seviour, T. W.; Marsili, E.; Loo, J. S. C.; Wuertz, S. Napthoquinone glycolysides for bioelectronalaytical enumeration of the faecal indicator Escherichia coli. *Microb. Biotechnol.* **2016**, *9*, 749-757.

20. Gooding, J. J. Biosensor technology for detecting biological warfare agents: Recent progress and future trends. *Anal. Chim. Acta*. **2006**, *559*, 137-151.

21. Zeiri, L.; Bronk, B. V.; Shabtai, Y.; Eichler, J.; Efrima, S. Surface-Enhanced Raman Spectroscopy as a Tool for Probing Specific Biochemical Components in Bacteria. *Appl. Spectrosc*. **2004**, *58*, 33-40.

22. Tao, F.; Peng, Y.; Xu, T. A rapid detection method of Escherichia coli by surface enhanced Raman scattering. *Proc. of SPIE*. **2015**, *9488*, 94880Q-1.

23. Liu, Y.; Chen, Y. R.; Nou, X.; Chao, K. Potential of Surface-Enhanced Raman Spectroscopy for the Rapid Identification of Escherichia Coli and Listeria Monocytogenes Cultures on Silver Colloidal Nanoparticles. *Appl. Spectrosc.* **2007**, *61*, 824-831.

24. Najafi, R.; Mukherjee, S.; Hudson Jr., J.; Sharma, A.; Banerjee, P. Development of a rapid capture-cum-detection method for *Escherichia coli* 0157 from apple juice comprising nano-immunomagnetic separation in tandem with surface enhanced Raman scattering. *Int. J. Food Microbiol.* **2014**, *189*, 89-97.

25. Gau, W.; Li, B.; Yao, R.; Li, Z.; Wang, X.; Dong, X, Qu, H.; Li, Q.; Li, N.; Chi, H.; Zhou, B.; Xia, Z. Intuitive Label-Free SERS Detection of Bacteria Using Aptamer-Based in Situ Silver Nanoparticle Synthesis. *Anal. Chem.* **2017**, *89*, 9836-9842.

26. Wang, J.; Wu, X.; Wang, C.; Shao, N.; Dong, P.; Xiao, R.; Wang, S. Magnetically Assisted Surface-Enhanced Raman Spectroscopy for the Detection of Staphylococcus aureus Based on Aptamer Recognition. *Appl. Mater. Interfaces*. **2015**, *7*, 20919-20929.

27. Knauer, M.; Ivleva, N. P.; Niessner, R.; Haisch, C. A flow-through microarray cell for the outline SERS detection of antibody-captured E. coli bacteria. *Anal. Bioanal. Chem.* **2012**, *402*, 2663-2667.

28. Chen, J.; Wu, X.; Huang, Y.-W.; Zhao, Y. Detection of *E. coli* using SERS active filters with silver nanorod array. *Sens. Actuators, B.* **2014**, *191*, 485-490.

29. Mosier-Boss, P.A.; Sorensen, K. C.; George, R. D.; Sims, P. C.; O'braztsova, A. SERS substrates fabricated using ceramic filters for the detection of bacteria: Eliminating the citrate interference. *Spectrochim. Acta A*. **2017**, *180*, 161-167.

30. Boardman, A. K.; Wong, W. S.; Premasiri, W. R.; Ziegler, L. D.; Lee, J. C.; Miljkovic, M.; Klapperich, C. M.; Sharon, A.; Sauer-Budge, A. F. Rapid Detection of Bacteria from Blood with Surface-Enhanced Raman Spectroscopy. *Anal. Chem.* **2016**, *88*, 8026-8035.

31. Jarvis, R. M.; Goodacre, R. Discrimination of Bacteria Using Surface-Enhanced Raman Spectroscopy. *Anal. Chem*. **2004**, *76*, 40-47.

32. Premasiri, W. R.; Chen, Y.; Williamson, P. M.; Bandarage, D.C.; Pyles, C.; Ziegler, L.D. Rapid urinary tract infection diagnostics by surface-enhanced Raman spectroscopy (SERS): identification and antibiotic susceptibilities. *Anal. Bioanal. Chem.* **2017**, *409*, 3043-3054.

33. El Badawy, A. M.; Silva, R. G.; Morris, B.; Scheckel, K. G.; Suidan, M. T.; Tolaymat, T. M. Surface Charge-Dependent Toxicity of Silver Nanoparticles. *Environ. Sci. Technol*. **2011**, *45*, 283-287.

34. Zhou, H.; Yang, D.; Ivleva, N. P.; Mircescu, N. E.; Schubert, S.; Niessner, R.; Wieser, A.; Haisch, C. Label-Free in Situ Discrimination of Live and Dead Bacteria by Surface-Enhanced Raman Scattering. *Anal. Chem.* **2015**, *87*, 6553-6561.

35. Marotta, N. E.; Bottomley, L. A. Surface-enhanced Raman scattering of bacterial cell culture growth media. *Appl. Spectrosc*. **2010**, *64*, 601-606.

36. Premasiri, W. R.; Gebregziabher, Y.; Ziegler, L. D. On the Difference Between Surface-Enhanced Raman Scattering (SERS) Spectra of Cell Growth Media and Whole Bacterial Cells. *Appl. Spectrosc.* **2001**, *65*, 493-499.

37. Raman, C. V.; Krishnan, K. S. A New Type of Secondary Radiation. *Nature*, **1928**, *121*, 501-502.

38. Kudelski, A. Analytical applications of Raman spectroscopy. Talanta, **2008**, *76*, 1-8.

39. Haynes, C. L.; McFarland, A. D.; Van Duyne, R. P. Surface-Enhanced Raman Spectroscopy. *Anal. Chem*. **2005**, *77*, 338A-346A.

40. Rycenga, M.; Cobley, C. M.; Zeng, J.; Li, W.; Moran, C. H.; Zhang, Q.; Qin, D.; Xia, Y. Controlling the Synthesis and Assembly of Silver Nanostructures for Plasmonic Applications. *Chem. Rev.* **2011**, *111*, 3669-3712.

41. Sharma, B.; Frontiera, R. R.; Henry, A. I.; Ringe, E.; Van Duyne, R. P. SERS: Materials, applications, and the future. *Mater. Today*, **2012**, *15*, 16-25.

42. Kneipp, K. Surface Enhanced Raman Scattering (SERS) of Nucleic Acids Adsorbed on Colloidal Silver Particles. *J. Mol. Struct.* **1986**, *145*, 173-179.

43. Brett, C. M. A.; Brett, A. M. O. *Electrochemistry Principles, Methods, and Applications*; Oxford University Press: New York, 1993.

44. Wang, J. *Analytical Electrochemistry*, 2nd ed.: Wiley-VCH: New York, 2000; pp 1-3, 100-103.

45. Grahame, D. C. The Electrical Double Layer and the Theory of Electrocapillarity. *Chem. Rev.* **1947**, *41*, 441-501.

46. Abdelsalam, M. E.; Bartlett, P. N.; Baumber, J. J.; Cintra, S.; Kelf, T. A.; Russell, A. Electrochemical SERS at a structured gold surface. *Electrochem. Commun.* **2005**, *7*, 740-744.

47. Robinson, A. M.; Harroun, S. G.; Bergman, J.; Brosseau C. L. Portable Electrochemical Surface-Enhanced Raman Spectroscopy System for Routine Spectroelectrochemical Analysis. *Anal. Chem.* **2012**, *84*, 1760-1764.

48. Wain, A. J.; O'Connell, M. A. Advances in surface-enhanced vibrational spectroscopy at electrochemical interfaces. *Adv. Phys.* **2017**, *2*, 188-209.

49. Lee, K. S.; El-Sayed, M. A. Gold and silver nanoparticles in sensing and imaging: sensitivity of plasmon response to size, shape, and metal composition. *J. Phys. Chem. B.* **2006**, *110*, 19220-19225.

50. Karaballi, R. A.; Merchant, S.; Power, S. R.; Brosseau, C. L. Electrochemical surface-enhanced Raman spectroscopy (EC-SERS) study of the interaction between protein aggregates and biomimetic membranes. *J. Phys. Chem. Chem. Phys.* **2018**, *20*, 4513-4526.

51. Huang, W.; Jiang, J. Z.; Chen, L.; Zhang, B. Q.; Deng, S. F.; Sun, J. J.; Chen, W. K. Density functional theory and surface enhanced Raman spectroscopy studies of tautomeric hypoxanthine and its adsorption behaviors in electrochemical processes. *Electrochimica Acta,* **2015**, *164*, 132-138.

52. You, L. X.; Liu, L. D.; Xiao, Y.; Dai, Y. F.; Chen, B. L.; Jiang, Y. X.; Zhao, F. Flavins mediate extracellular electron transfer in Gram-positive *Bacillus Megaterium* strain LLD-1. *Bioelectrochem.* **2018**, *119*, 196-202.

53. Pagliai, M.; Caporali, S.; Muniz-Miranda, M.; Pratesi, G.; Schettino, V. SERS, XPS, and DFT Study of Adenine Adsorption on Silver and Gold Surfaces. *J. Phys. Chem. Lett.* **2012**, *3*, 242-245.

54. Madzhorva, F.; Heiner, Z.; Guhlke, M.; Kneipp, J. Surface-Enhanced Hyper-Raman Spectra of Adenine, Guanine, Cytosine, Thymine, and Uracil. *J. Phys. Chem. C.* **2016**, *120*, 15415-15423.

55. Zhao, L.; Blackburn, J.; Brosseau, C. L. Quantitative Detection of Uric Acid by Electrochemical-Surface Enhanced Raman Spectroscopy Using a Multilayered Au/Ag Substrate. *Anal. Chem.* **2015**, *87*, 441-447.

Appendix

Before beginning to use phosphate buffer as an electrolyte, it was important to establish that it would have no interfering EC-SERS signal. Figure A1 shows the EC-SERS in air, OCP cathodic, -1.0 V, and OCP anodic spectra for phosphate buffer under all three possible set-ups for EC-SERS (Ag 780, Ag 532, and Au 780). The "In Air" spectra are of a bare electrode that has been treated with KCl. The rest of the spectra were collected as described in the results section for EC-SERS measurements after the addition of phosphate buffer.
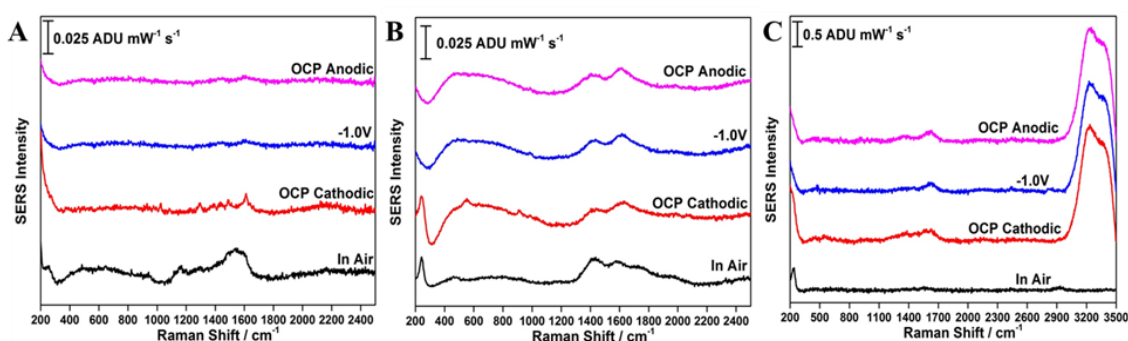
Figure A1: (A) EC-SERS of phosphate buffer on gold collected with an excitation wavelength of 780 nm, (B) EC-SERS of phosphate buffer on silver collected with an excitation wavelength of 780 nm, and (C) EC-SERS of phosphate buffer on silver collected with an excitation wavelength of 532 nm.

As the SERS spectra for bacteria have been shown to be attributed to the nucleotide breakdown products adenine, hypoxanthine, xanthine, guanine, uric acid, AMP and guanosine, it was vital to establish reference EC-SERS data for all seven molecules. The data for each molecule using a silver substrate and a 532 nm excitation wavelength and using a gold substrate and a 780 nm excitation wavelength is shown in Figures A2-A15, as only silver substrates with a 780 nm excitation wavelength were used for bacterial screening. Note that the data for guanine and uric on gold (780 nm laser) have

been excluded due to their irreproducibility and noisy spectra. All spectra collected using the 780 nm excitation laser line were collected with a laser power of 80 mW with an acquisition time of 30 seconds, and all spectra collected using the 532 nm excitation laser line were collected with a laser power of 3 mW with an acquisition time of 30 seconds.
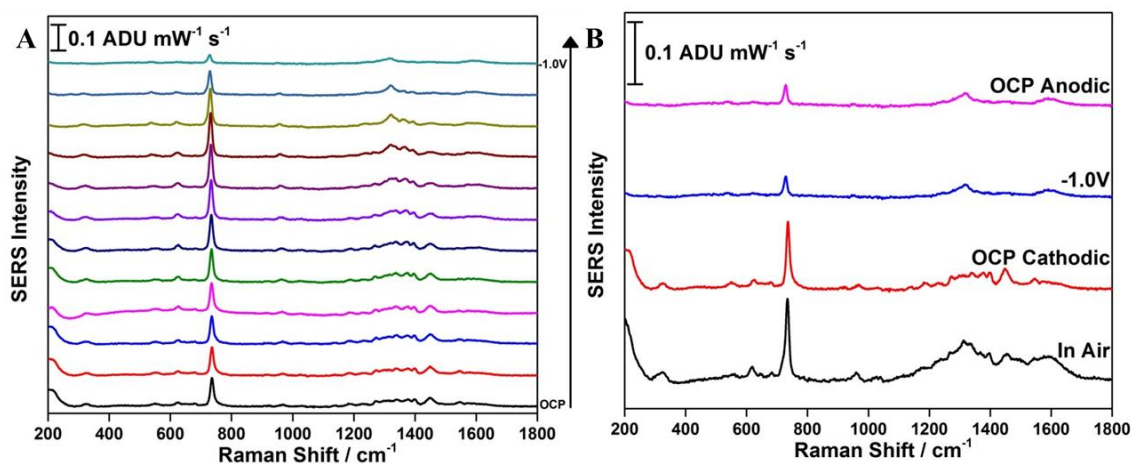

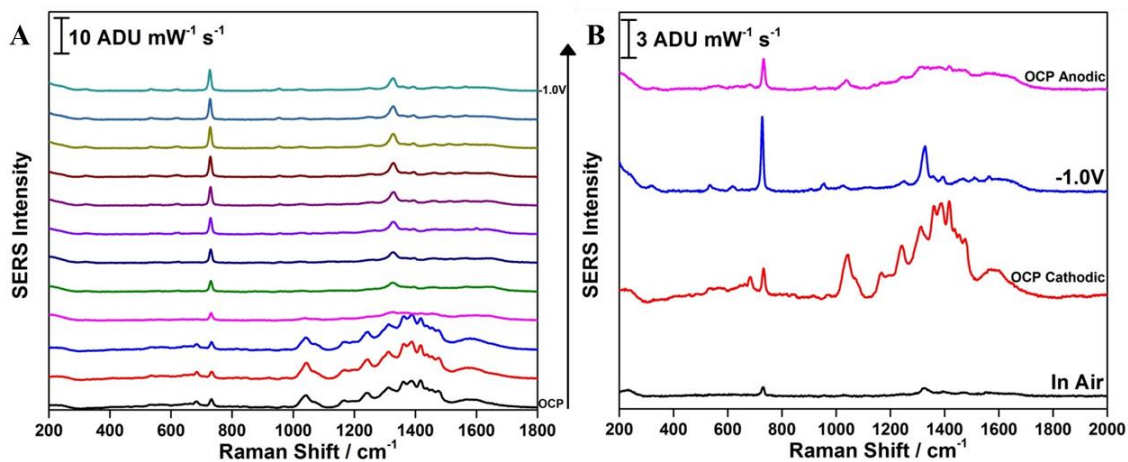**Figure A2:** (A) Cathodic progression of the SERS spectra and (B) EC-SERS comparison for adenine on gold using an excitation wavelength of 780 nm.

Figure A3: (A) Cathodic progression of the SERS spectra and (B) EC-SERS comparison for adenine on gold using an excitation wavelength of 532 nm.
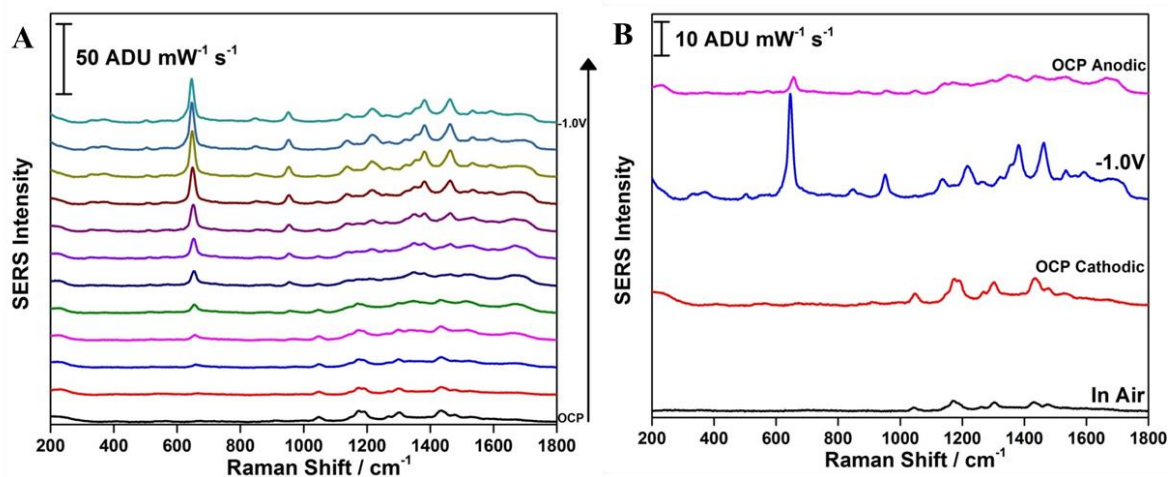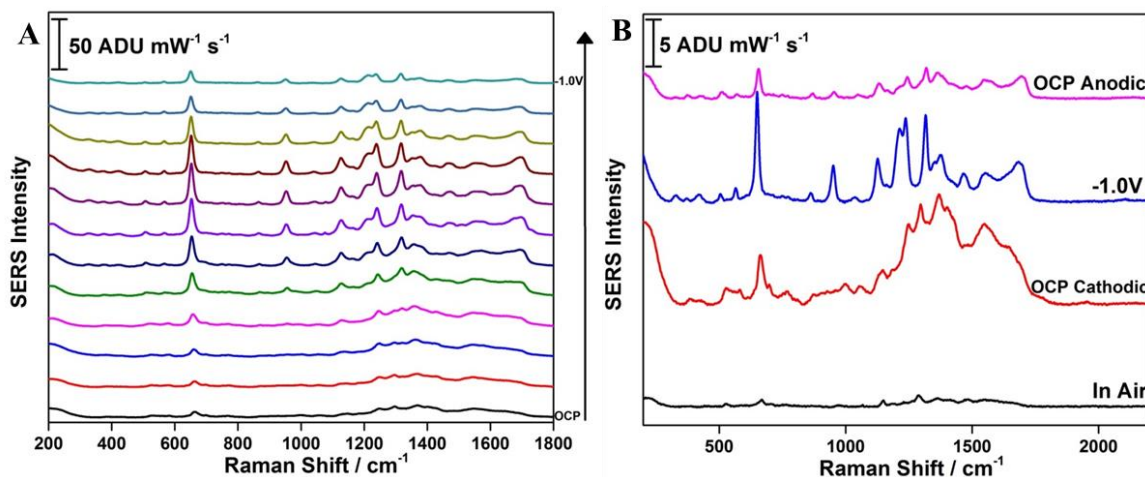
Figure A4: (A) Cathodic progression of the SERS spectra and (B) EC-SERS comparison for guanine on silver using an excitation wavelength of 532 nm.
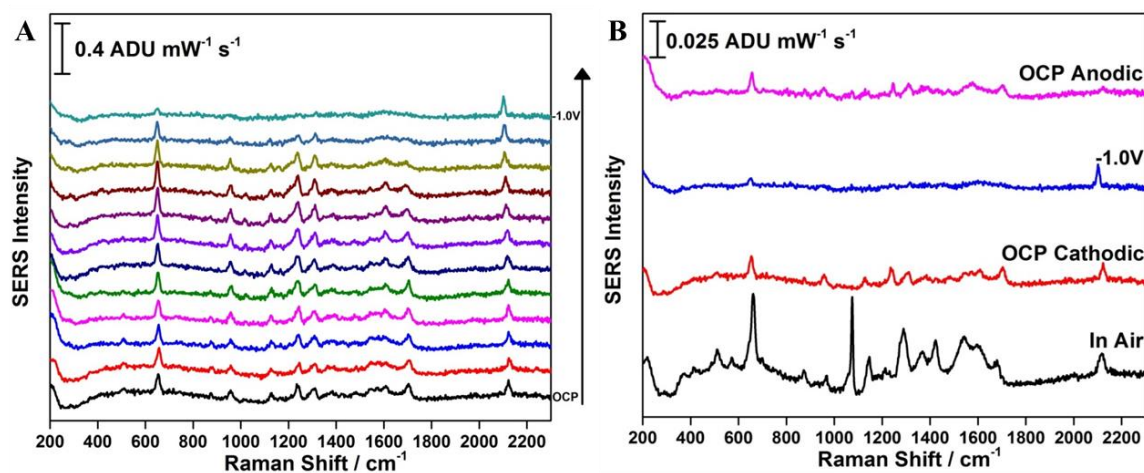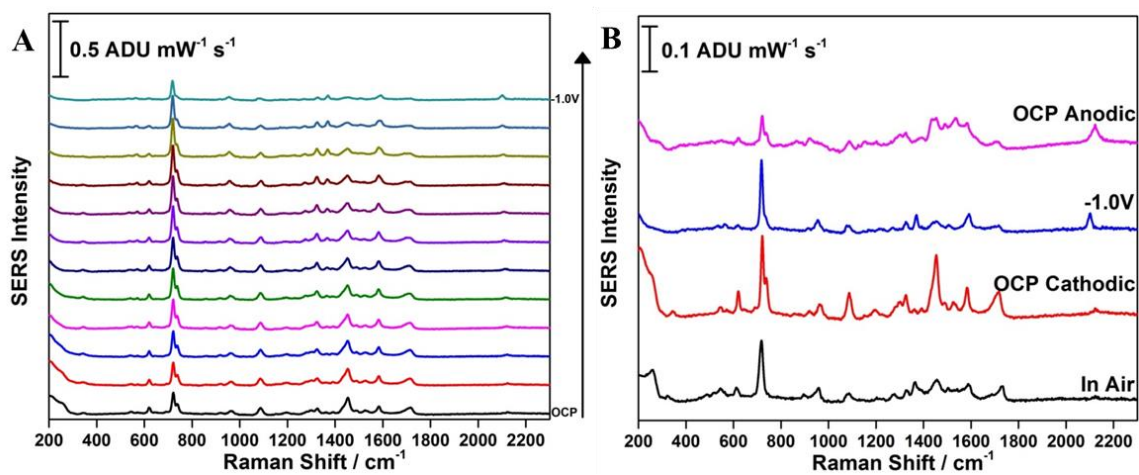

Figure A5: (A) Cathodic progression of the SERS spectra and (B) EC-SERS comparison for xanthine on gold using an excitation wavelength of 780 nm.
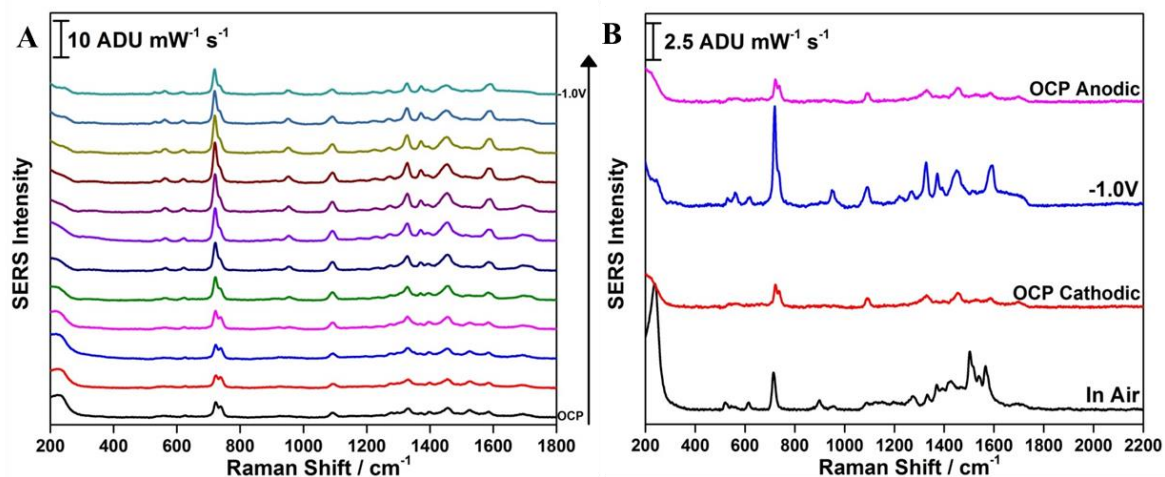
Figure A6: (A) Cathodic progression of the SERS spectra and (B) EC-SERS comparison for xanthine on silver using an excitation wavelength of 532 nm.
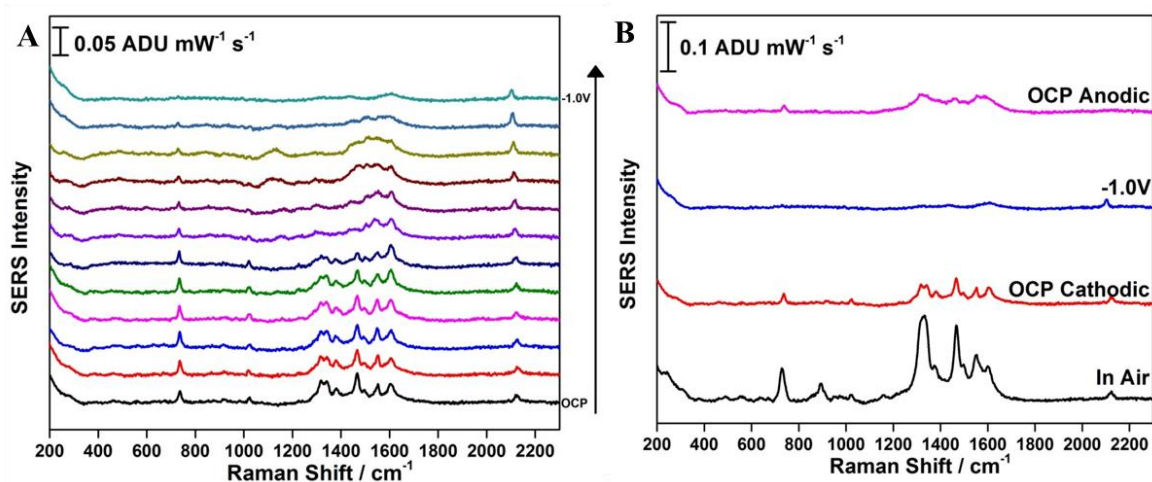

Figure A7: (A) Cathodic progression of the SERS spectra and (B) EC-SERS comparison for hypoxanthine on gold using an excitation wavelength of 780 nm.

Figure A8: (A) Cathodic progression of the SERS spectra and (B) EC-SERS comparison for hypoxanthine on silver using an excitation wavelength of 532 nm.

Figure A9: (A) Cathodic progression of the SERS spectra and (B) EC-SERS comparison for AMP on gold using an excitation wavelength of 780 nm.
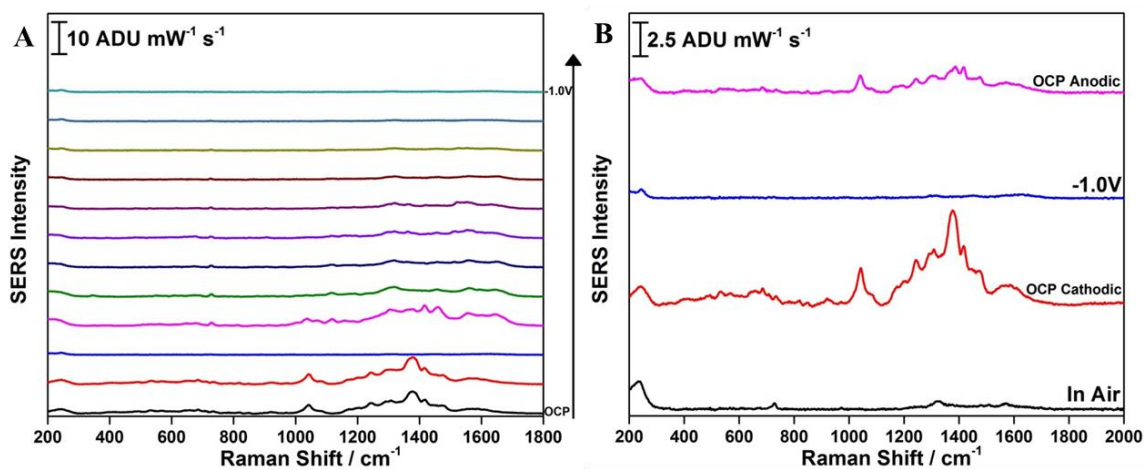
Figure A10: (A) Cathodic progression of the SERS spectra and (B) EC-SERS comparison for AMP on silver using an excitation wavelength of 532 nm.
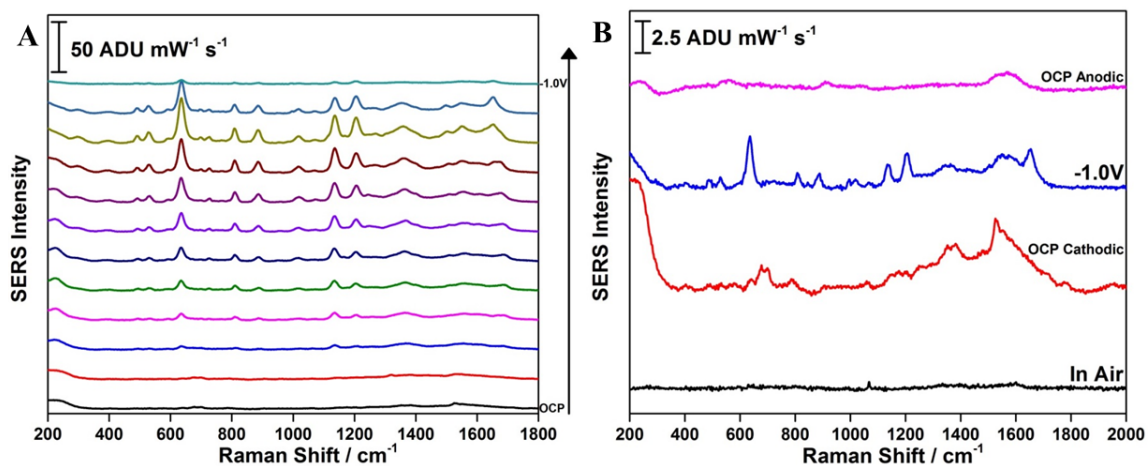

Figure A11: (A) Cathodic progression of the SERS spectra and (B) EC-SERS comparison for uric acid on silver using an excitation wavelength of 532 nm.
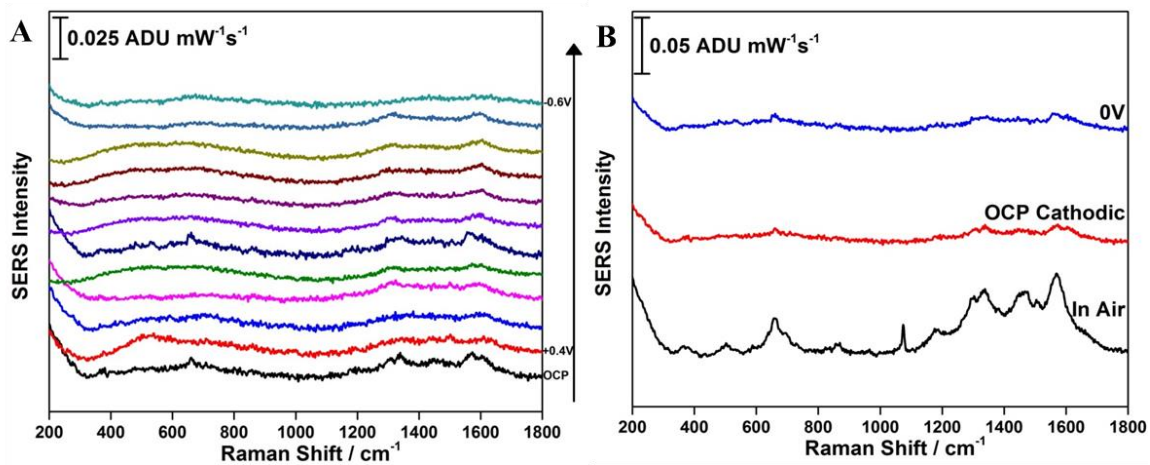
Figure A12: (A) Cathodic progression of the SERS spectra and (B) EC-SERS comparison for guanosine on gold using an excitation wavelength of 780 nm.
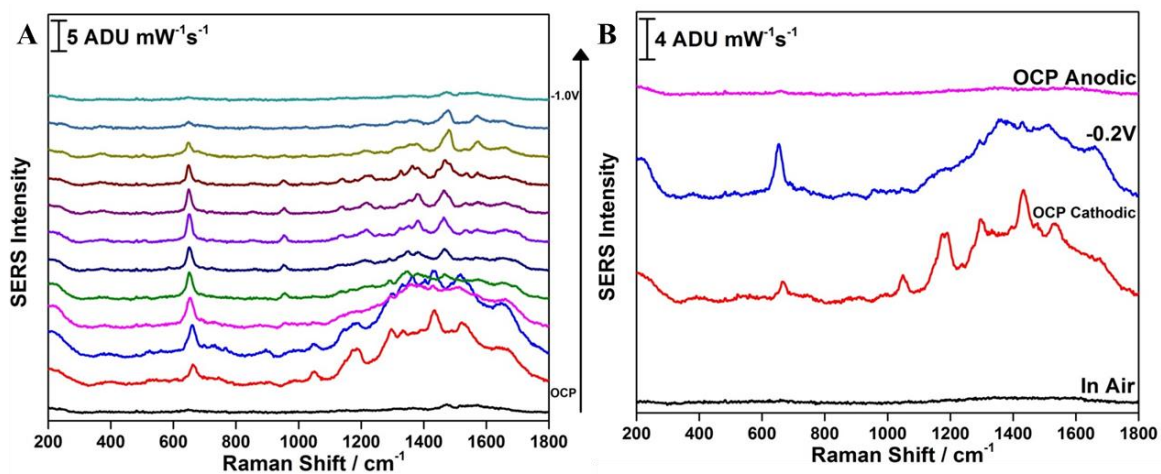

Figure A13: (A) Cathodic progression of the SERS spectra and (B) EC-SERS comparison for guanosine on silver using an excitation wavelength of 532 nm.
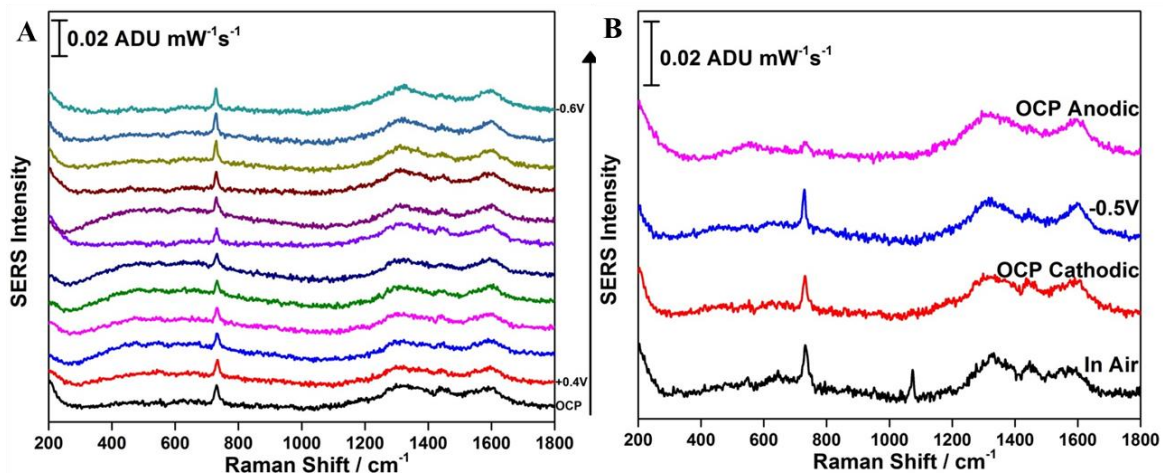
Figure A14: (A) Cathodic progression of the SERS spectra and (B) EC-SERS comparison for mixture of all seven breakdown products on gold using an excitation wavelength of 780 nm.
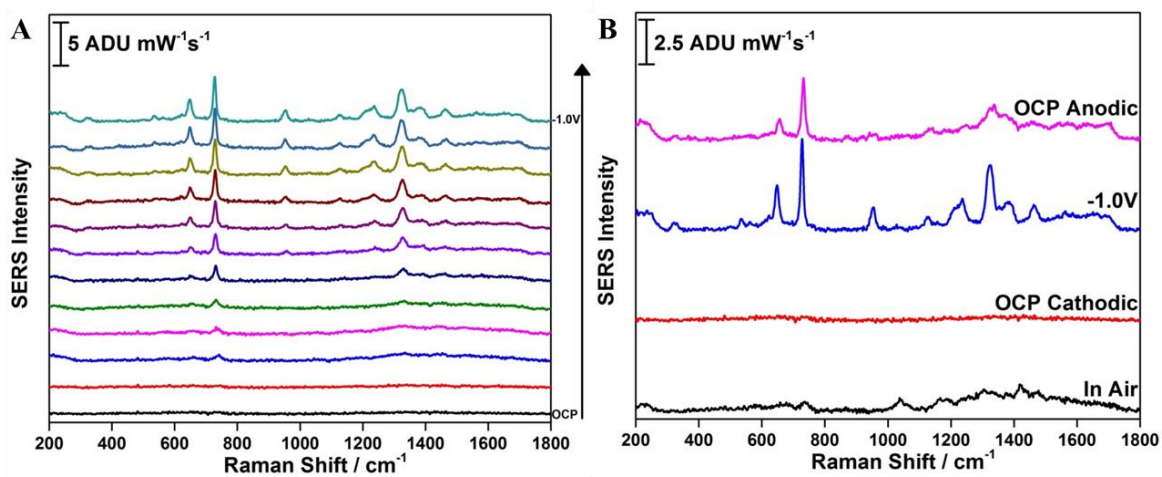

Figure A15: (A) Cathodic progression of the SERS spectra and (B) EC-SERS comparison for mixture of all seven breakdown products on silver using an excitation wavelength of 532 nm.
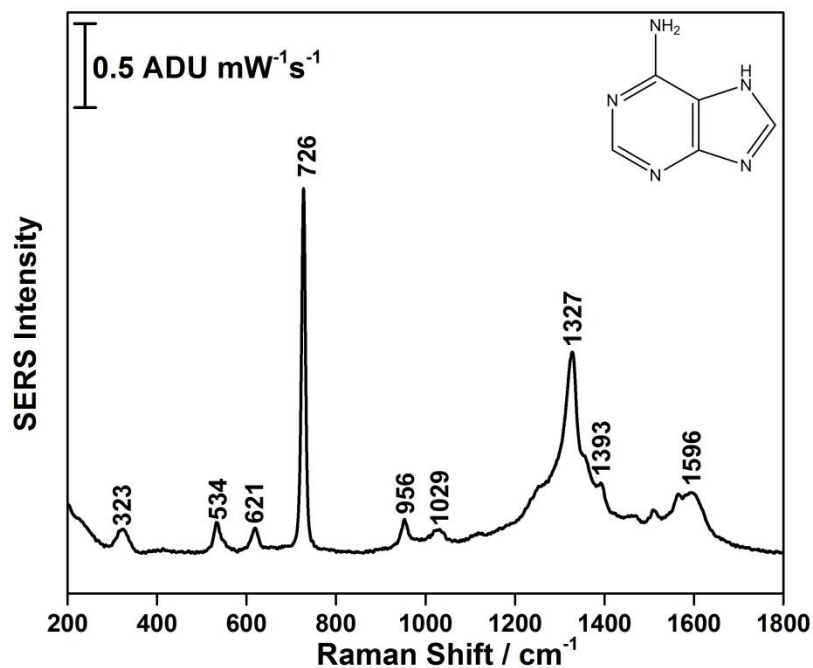
Figure A16: Optimized negative SERS spectrum of adenine (-1.0 V) on silver using the 780 nm excitation laser line with labelled peaks. Laser power was 80 mW and acquisition time was 30 seconds.

Table A1: Peaks present in the SERS spectrum of adenine adsorbed on silver using the 780 nm laser line.[54,55]

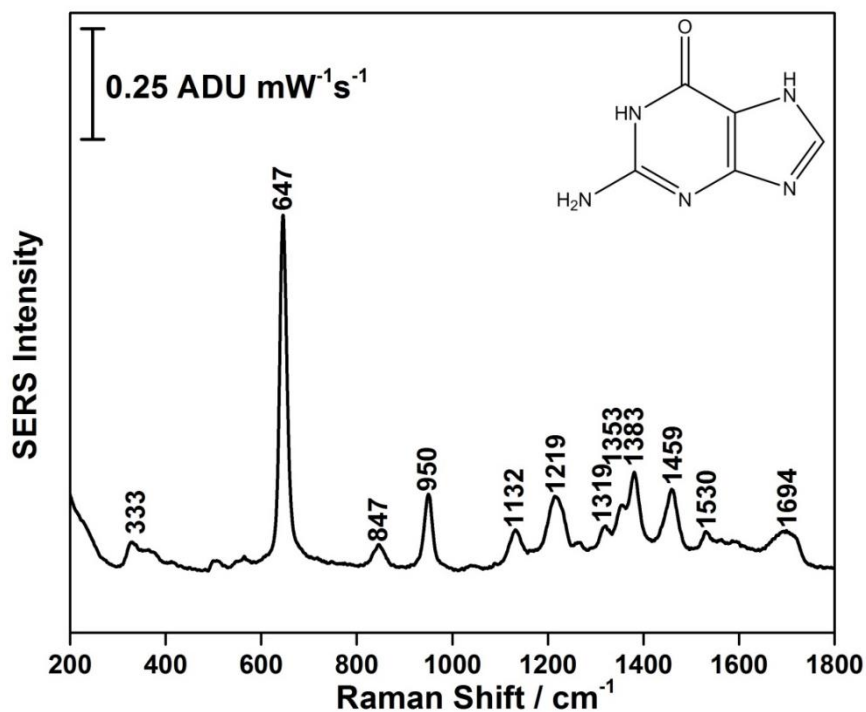| Peak (cm^{-1})	Assignment
323	-
534	C-H and N-H wagging
621	Ring deformations
726	Ring breathing
956	Ring deformations
1029	NH$_2$ rocking
1327	H bending and ring stretching
1393	H bending and ring stretching
1596	Ring stretching

Figure A17: Optimized negative SERS spectrum of guanine (-1.0 V) on silver using the 780 nm excitation laser line with labelled peaks. Laser power was 80 mW and acquisition time was 30 seconds.

Table A2: Peaks present in the SERS spectrum of guanine adsorbed on silver using the 780 nm laser line.[55]

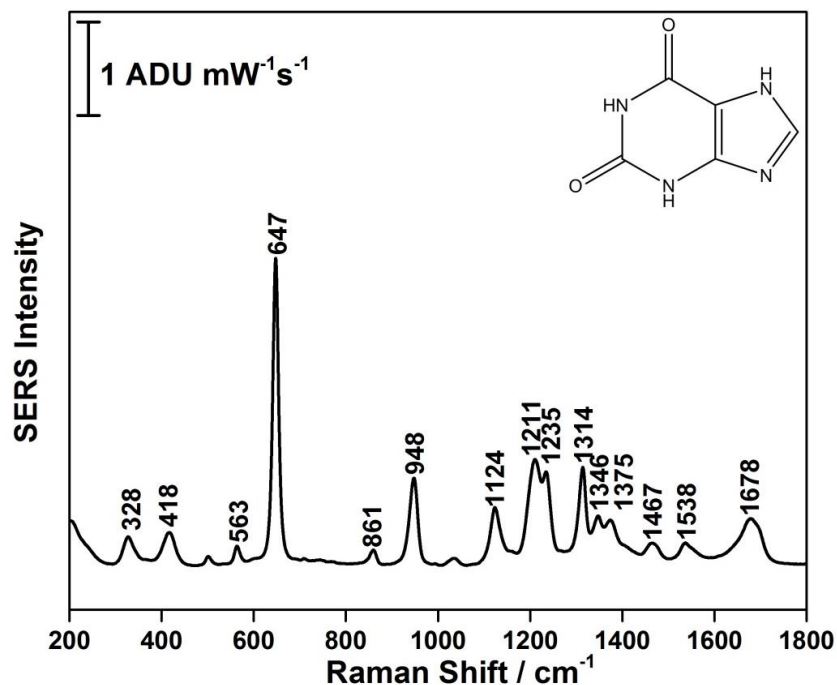| Peak (cm^{-1})	Assignment
333	-
647	Guanine ring breathing mode
847	-
950	C-C stretch backbone
1132	Symmetric stretch of backbone
1219	-
1319	-
1353	N-H bending, C-N stretching
1383	C-N ring stretching, NH_2 rocking, N-H bending
1459	C-N ring stretching, C-H and N-H bending
1530	C-N ring stretching C-N, N-H bending
1694	C=O stretching, N-H bending, NH_2 scissoring

Figure A18: Optimized negative SERS spectrum of xanthine (-1.0 V) on silver using the 780 nm excitation laser line with labelled peaks. Laser power was 80 mW and acquisition time was 30 seconds.

Table A3: Peaks present in the SERS spectrum of xanthine adsorbed on silver using the 780 nm laser line.[52]

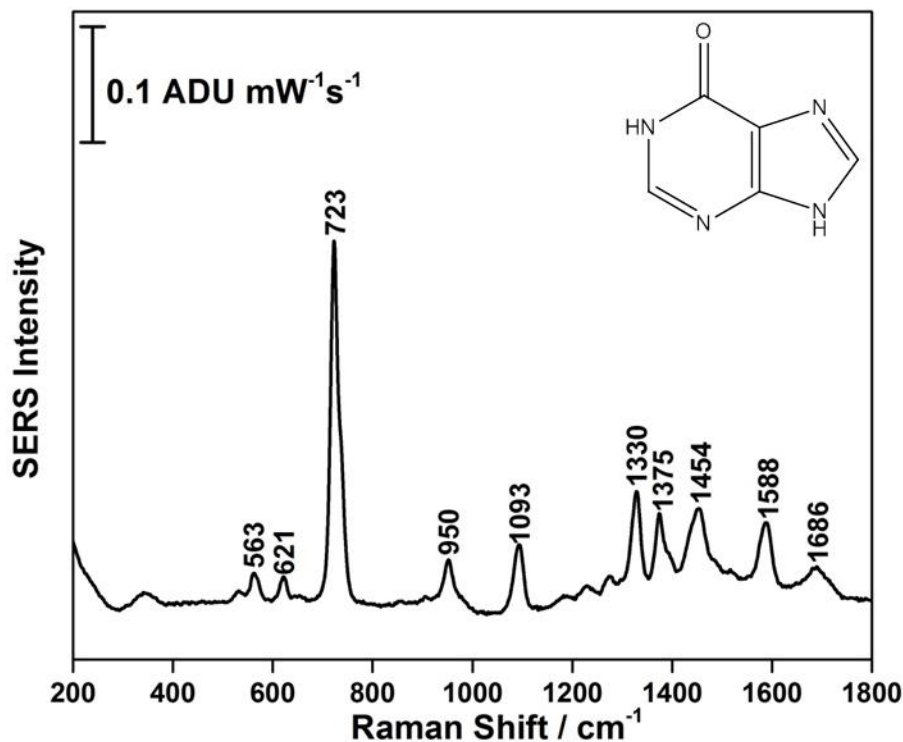| Peak (cm^{-1})	Assignment
328	-
418	-
563	Ring deformations
647	Ring breathing
861	-
948	Pyrimidine ring breathing
1124	-
1211	-
1235	C-H rocking
1314	-
1346	C-H rocking
1375	C-H rocking, imidazole ring breathing
1467	C-H, N-H rocking and imidazole ring
1538	N=C stretching, pyrimidine ring stretching
1678	C=O stretching

Figure A19: Optimized negative SERS spectrum of hypoxanthine (-1.0 V) on silver using the 780 nm excitation laser line with labelled peaks. Laser power was 80 mW and acquisition time was 30 seconds.

Table A4: Peaks present in the SERS spectrum of hypoxanthine adsorbed on silver using the 780 nm laser line.[52]

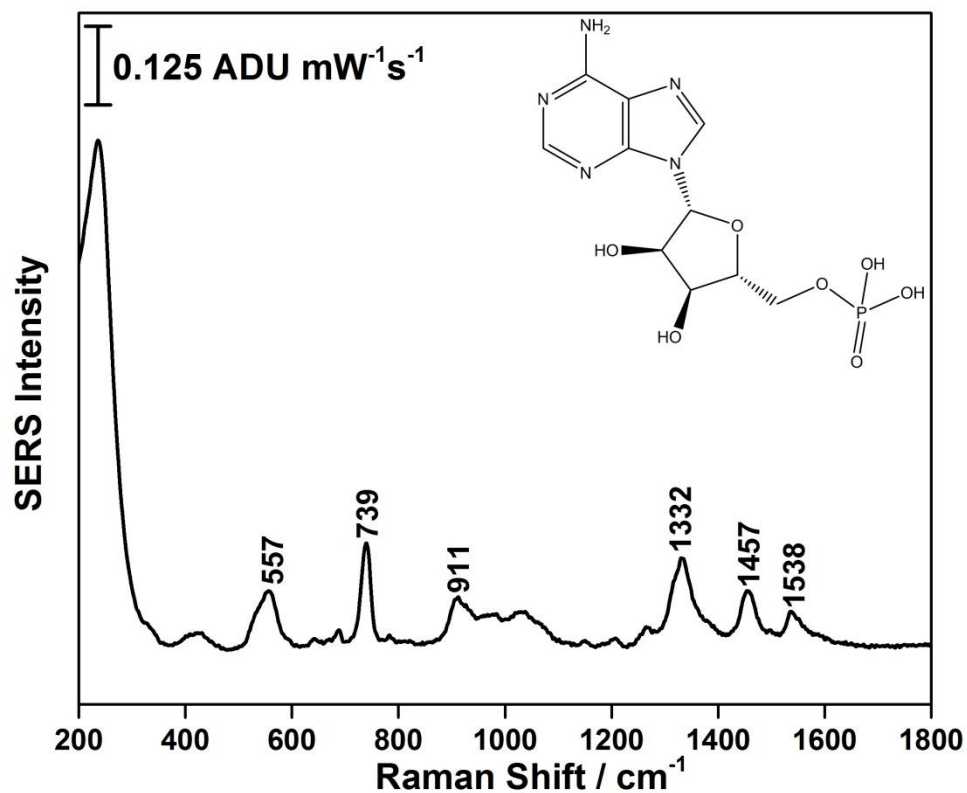| Peak (cm^{-1})	Assignment
563	Ring deformations
621	Ring breathing
723	Purine ring breathing
950	Pyrimidine ring breathing
1093	Symmetric stretch of backbone
1330	C-H rocking
1375	C-H rocking, imidazole ring breathing
1454	C-H, N-H rocking and imidazole ring deformations
1588	N=C stretching, pyrimidine ring stretching
1686	C=O stretching

Figure A20: Optimized negative SERS spectrum of AMP (0 V) on silver using the 780 nm excitation laser line with labelled peaks. Laser power was 80 mW and acquisition time was 30 seconds.

Table A5: Peaks present in the SERS spectrum of AMP adsorbed on silver using the 780 nm laser line.[54,55]

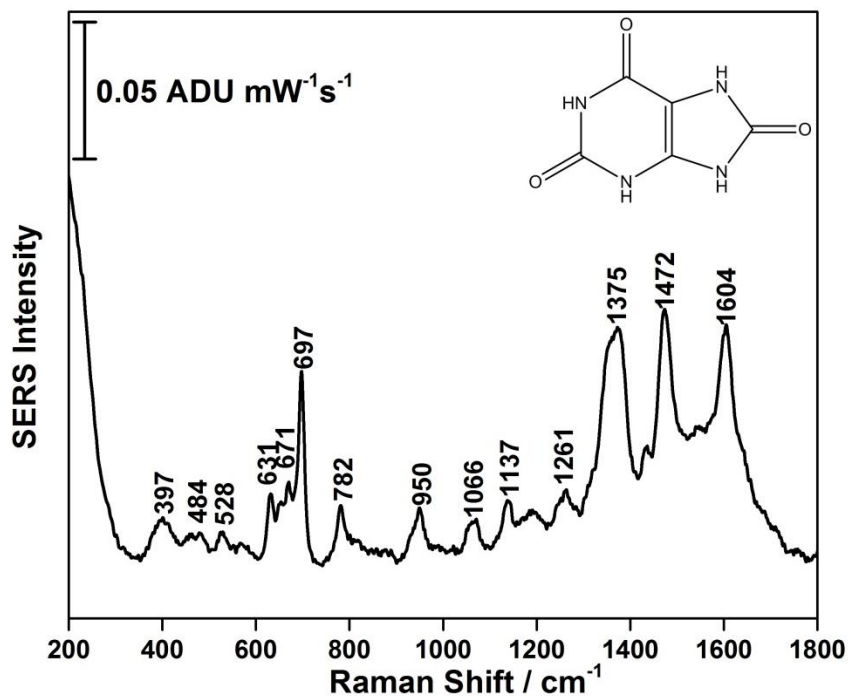| Peak (cm⁻¹)	Assignment
557	C-H and C-H wagging
739	Ring breathing
911	Ring deformations
1332	H bending and ring stretching
1457	C-H bending
1538	-

Figure A21: Optimized negative SERS spectrum of uric acid (-0.5 V) on silver using the 780 nm excitation laser line with labelled peaks. Laser power was 80 mW and acquisition time was 30 seconds.

Table A6: Peaks present in the SERS spectrum of uric acid adsorbed on silver using the 780 nm laser line.[56]

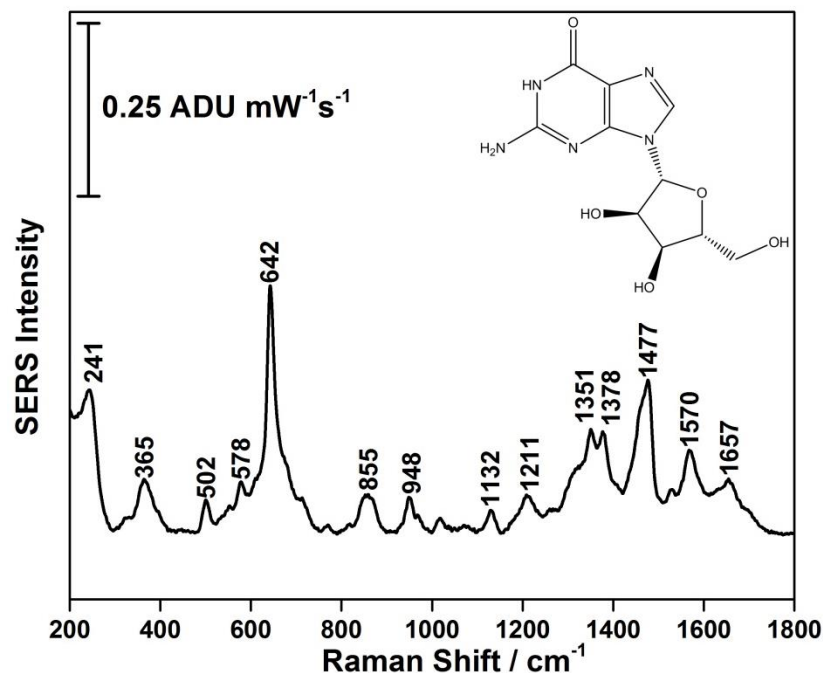| Peak (cm^{-1})	Assignment
397	-
484	C-N-C ring vibrations
528	
631	Skeletal ring deformation
671	-
697	-
782	-
950	-
1066	Mixed vibrations: ring vibrations, C-O, C-C, C-N, N-C-C stretching and bending
1137	
1261	
1375	
1472	-
1604	C-N stretching

Figure A22: Optimized negative SERS spectrum of guanosine (-0.8 V) on silver using the 780 nm excitation laser line with labelled peaks. Laser power was 80 mW and acquisition time was 30 seconds.

Table A7: Peaks present in the SERS spectrum of guanosine adsorbed on silver using the 780 nm laser line.[55]

Peak (cm^{-1})	Assignment
241	Ag-Cl
365	-
502	-
578	-
642	Guanine ring breathing mode
855	-
948	C-C stretch backbone
1132	Symmetric stretch of backbone
1211	-
1351	N-H bending, C-N stretching
1378	C-N ring stretching, NH$_2$ rocking, N-H bending
1477	C-H bending
1570	Amide II
1657	Amide I